frontiers | Frontiers in Ecology and Evolution

TYPE Original Research
PUBLISHED 03 October 2024
DOI 10.3389/fevo.2024.1445160

OPEN ACCESS

EDITED BY
Paulo Tarso Freire,
Federal University of Ceara, Brazil

REVIEWED BY
Michal Kowalewski,
University of Florida, United States
Pedro Façanha,
Federal University of Maranhão, Brazil

*CORRESPONDENCE
Arianny P. Storari
ariannystorari@gmail.com

RECEIVED 06 June 2024
ACCEPTED 05 September 2024
PUBLISHED 03 October 2024

CITATION
Storari AP, Osés GL, Staniczek AH, Rizzutto M, Loeffler R and Rodrigues T (2024) Paleometric approaches reveal striking differences in the insect fossilization of two Mesozoic Konservat-Lagerstätten. *Front. Ecol. Evol.* 12:1445160. doi: 10.3389/fevo.2024.1445160

Paleometric approaches reveal striking differences in the insect fossilization of two Mesozoic Konservat-Lagerstätten

Arianny P. Storari[1]*, Gabriel L. Osés[2,3], Arnold H. Staniczek[4], Marcia Rizzutto[2], Ronny Loeffler[5] and Taissa Rodrigues[1]

[1]Laboratório de Paleontologia, Departamento de Ciências Biológicas, Centro de Ciências Humanas e Naturais, Universidade Federal do Espírito Santo (UFES), Vitória, ES, Brazil, [2]Laboratório de Arqueometria e Ciências Aplicadas ao Patrimônio Cultural, Instituto de Física, Universidade de São Paulo (USP), São Paulo, SP, Brazil, [3]Programa de Pós-Doutorado, Instituto de Física, Universidade de São Paulo (USP), São Paulo, SP, Brazil, [4]Department of Entomology, State Museum of Natural History, Stuttgart, Germany, [5]Center for Light-Matter Interaction, Sensors and Analytics (LISA+), Eberhard Karls University Tübingen, Tübingen, Germany

The Crato Formation (Lower Cretaceous, Brazil) is a Konservat-Lagerstätte preserving a great number of exceptionally well-preserved insects. Here, we sought to explore the preservational modes of two abundant aquatic and terrestrial groups of this unit, mayflies and crickets. To better understand how exceptional is their preservation, we also present detailed data on the modes of preservation of mayflies from the renowned Solnhofen limestones (Upper Jurassic, Germany). For the Crato Formation, out of 234 fossil mayflies and crickets, ten specimens were additionally analyzed using scanning electron microscopy coupled to energy dispersive X-ray spectroscopy (SEM-EDS), energy and micro-energy dispersive X-ray fluorescence (EDXRF and μEDXRF), and μRaman spectroscopy. For the Solnhofen limestones, 85 adult mayflies were analyzed, and five of them were subjected to SEM-EDS and μEDXRF analyses. The Crato specimens preserve several external and internal microfeatures. The areas with the highest fidelity of preservation are characterized by smaller and more closely-packed crystals when compared to less-preserved parts. We also recovered microscopic features that suggest the presence of microbial mats during the fossilization process. All the analyzed Crato specimens are preserved by replacement of tissues with iron oxides after pyritization. Sulfur occurs scattered in some regions of the crickets, but is associated with low iron counts, which may indicate the presence of sulfates post-dating pyrite oxidation. Additionally, the orthopterans have calcium phosphate preserving some of their structures. Differing from Crato insects, Solnhofen mayflies are overall poorly preserved as mere imprints, and their micron-scale morphology is obliterated by coarse mineral growth, whereas tissues are obliterated by calcite crystals alone or in combination with globular material. There is an elevated concentration of Si, K, Ca, Ti, Mn, and Fe in comparison to the host rock, which may be related to a yet unknown mineral phase(s). Although the paleoenvironments of the Crato Formation and the Solnhofen limestones are different, there are similarities in the style of preservation of their vertebrates and

in some of their paleoenvironmental conditions such as anoxic hypersaline bottom waters and deposition of laminated limestones. However, the same does not apply to the preservation of insects, specifically mayflies, which are poorly preserved in the Solnhofen limestones.

KEYWORDS

paleoentomology, insect taphonomy, Crato Formation, Solnhofen, Ephemeroptera, Orthoptera

1 Introduction

Most exceptionally preserved insect biotas are restricted to the Cenozoic, with a variety of preservational modes occurring, like calcification, phosphatization, silicification, and specimens preserved as gypsum crystals (Leakey, 1952; Palmer, 1957; Duncan and Briggs, 1996; Duncan et al., 1998; McCobb et al., 1998; Schlüter et al., 2002; Parker and McKenzie, 2003; Wappler and Ben-Dov, 2008; Schwermann et al., 2016). However, although less frequent than in the Cenozoic, there are many important insect biotas in the Mesozoic. An example is the renowned Crato Formation of Brazil which, in most of its reported cases, preserves insects by phosphatization or pyritization (Dias and Carvalho, 2022). Calcium phosphate is commonly known to replicate soft tissues since Precambrian times, and it is often associated with Lagerstätten (Wilby and Briggs, 1997; Martínez-Delclòs et al., 2004; Eriksson et al., 2012; Chen et al., 2014). The preservational fidelity of phosphatized fossils is achieved by calcium phosphate impregnation of soft tissues, attributed to bacterial precipitation, although it has been observed that arthropod carcasses can supply enough phosphate for mineralization of their own tissues (Briggs et al., 1993; Martínez-Delclòs et al., 2004; Maas et al., 2006). Pyrite, however, is less frequent in comparison to other types of mineral replacements, and in most cases does not replicate soft tissues with the same fidelity as calcium phosphate, with one of the exceptions being the Crato Formation fossils (Osés et al., 2016).

The Lower Cretaceous (Upper Aptian) Crato Formation is regarded as one of the most important Mesozoic Lagerstätten. It is widely accepted that this unit, known for its laminated limestones locally called "pedra cariri", represents a lacustrine past ecosystem. However, there are contrasting hypotheses regarding the salinity of its past waters, either supporting a brackish or more saline paleolake (episodically and/or in certain strata of the water body), or an exclusive freshwater setting (Grimaldi, 1990; Martill and Wilby, 1993; Neumann et al., 2003; Martill et al., 2007, 2008; Heimhofer et al., 2010; Barling et al., 2015, 2020, 2021; Oliveira and Kellner, 2017; Warren et al., 2016; Varejão et al., 2019; Moura-Júnior et al., 2020; Ribeiro et al., 2021; Storari et al., 2021a). This lithostratigraphic unit is of worldwide importance due to its outstanding fossil record, particularly preserving a great number of various insect taxa (Martins-Neto, 2005; Assine et al., 2014). Several publications already explored the taphonomy of the entomofauna from the Crato Formation, with studies varying from general remarks (Martínez-Delclòs et al., 2004), to detailed preservational analyses, including studies of certain processes affecting the preservation of insects like the action of microbial mats or weathering (Menon and Martill, 2007; Barling et al., 2015, 2020; Osés et al., 2016; Prado et al., 2021; Bezerra et al., 2021; Iniesto et al., 2021; Ribeiro et al., 2021; Dias and Carvalho, 2022; Bezerra et al., 2023). Detailed analyses including specific groups of insects are also available, as with cockroaches (Bezerra et al., 2018), crickets (Bezerra et al., 2020; Dias and Carvalho, 2020; Storari et al., 2024), odonatans (Nel and Pouillon, 2020; Pouillon and Nel, 2020; Barling et al., 2021), hemipterans (Moura-Júnior et al., 2020), beetles (Santos et al., 2021), and mayflies (Staniczek et al., 2022; Storari et al., 2021a; Dias et al., 2023).

Like the Crato Formation, many other fossiliferous units with finely laminated carbonates also preserve a diverse fossil insect assemblage, as the Solnhofen limestones of Germany, the Las Hoyas and Montsec localities of Spain, and the Green River Formation of the USA (Bezerra et al., 2020). In particular, the Solnhofen limestones *sensu stricto* of the Upper Jurassic of southern Germany, state of Bavaria, is arguably one of the most famous fossil Lagerstätten due to the iconic theropod *Archaeopteryx* and represents a past marine environment (Barthel et al., 1990). From the terrestrial fossils recovered there, insects are among the most diverse groups (Bechly, 2015), with eleven orders described so far, although some taxa still await further investigation and interpretation (Barthel et al., 1990). While excellent preservation of fossils is commonly reported for vertebrates, with soft parts such as the skin or feathers preserved (Frey et al., 2003; Tischlinger and Unwin, 2004), preservation of their insects is not well-studied, being discussed only in general bibliographies, or briefly cited either as examples of exceptional preservation or as poorly-preserved specimens (Ponomarenko, 1985; Barthel et al., 1990; Frickhinger, 1994, 1999; Martínez-Delclòs et al., 2004; Wang et al., 2010; Bechly, 2015).

The Crato Formation and the Solnhofen limestones are well-known deposits that, although differing in their paleoenvironmental settings, include exceptionally preserved fossils in laminated limestones, and interestingly vertebrates of both units share phosphatization as the main preservation type of their soft tissues (Martínez-Delclòs et al., 2004; Fielding et al., 2005; Gobbo and

Bertini, 2013; Warren et al., 2016; Varejão et al., 2019). Thus, we sought to analyze if the invertebrates from these deposits also share similar modes of preservation. We studied primarily insects of the Crato Formation, focusing on two abundant aquatic and terrestrial groups of this unit, Ephemeroptera and Orthoptera. For the comparison, we studied in detail the modes of preservation of mayflies from the Solnhofen limestones. The fossils are here analyzed under a paleometric approach. Paleometry is the study of ancient life using analytical techniques (quantitative or qualitative non-destructive) combining traditional tools from physics and chemistry within the field of paleontology (Delgado et al., 2014; Gomes et al., 2019).

2 Materials and methods

2.1 Geological setting

2.1.1 Crato Formation

The Araripe Basin is an intracratonic basin located in northeast Brazil, covering the states of Piauí, Pernambuco, and Ceará (Saraiva et al., 2021) (Figure 1). The base of this area is of Precambrian age and was affected over time by extensive rifting processes resulting from the split between Africa and South America during the break-up of Pangaea (Assine, 2007). The Araripe Basin is composed of several units, the oldest being the Cariri Formation, from the Late Ordovician/Early Devonian (*sensu* Beurlen, 1962), followed by the Brejo Santo and Missão Velha formations from the Upper Jurassic (pre-rift sequence), and the Abaiara Formation from Lower Cretaceous (rift sequence) (Assine et al., 2014). The subsequent Lower Cretaceous deposits of the basin are collectively known as the Santana Group (post-rift I sequence) (Figure 1). Finally, the basin cycle ends with its post-rift II sequence of the Araripina and Exu formations (Assine et al., 2014).

The Santana Group is subdivided, from bottom to top, into the Barbalha, Crato, Ipubi, and Romualdo formations (Neumann and Cabrera, 1999; Assine et al., 2014). The Crato Formation is interpreted as Late Aptian based on biostratigraphic data (Arai and Assine, 2020; Melo et al., 2020; Coimbra and Freire, 2021; Varejão et al., 2021). It is a ca. 90 m thick succession formed by horizontal strata of micritic limestone that are interbedded with shales, siltstones, and sandstones (Neumann and Cabrera, 1999; Assine et al., 2014; Catto et al., 2016). Most of its outcrops are exposed in commercial quarries, particularly between the Nova Olinda and Santana do Cariri municipalities, as well as on the Batateiras River banks, all located in the state of Ceará (Viana and Neumann, 2002) (Figure 1). Due to the absence of bioturbation and true marine fossils, there is strong indication that the Crato Formation strata were deposited under calm lacustrine conditions (Neumann et al., 2003; Heimhofer et al., 2010; Varejão et al., 2021; Ribeiro et al., 2021), though the presence of halite pseudomorphs and stromatolites in some sections suggests that the basin experienced salinity variations with increased arid and evaporitic conditions (Martill et al., 2007; Heimhofer et al., 2010; Warren et al., 2016; Storari et al., 2021a; Varejão et al., 2021).

The Crato Formation is divided into four members, namely, Nova Olinda, Caldas, Jamacaru, and Casa de Pedra, from bottom to top. The Nova Olinda Member holds the well-preserved fossils of the formation (Assine, 2007), and is where the fossil insects from this study were found. Additionally to this traditional grouping in members, the strata of the Crato Formation have received several classifications. Neumann et al. (2003) divided its carbonate facies into two sub-facies: clay-carbonate rhythmites and laminated limestones. Often, the first yields dark-gray-colored layers, while the latter corresponds to yellow-colored layers. More recently, Varejão et al. (2021) discussed that the Crato Formation encompasses six facies associations (FA-3 to FA-8), in which the exceptionally preserved fossils occur at the facies association 4 (FA-4), with insects usually found in its upper layers (Varejão et al., 2021). A previous classification by Varejão et al. (2019) pointed out that the stratigraphic position of most insects is a layer called Interval III, consisting of the upper 2-meter part of the Lagerstätte succession (Nova Olinda Member). Finally, the Crato Formation has also been divided into six carbonate intervals, designated C1 to C6 by Neumann and Cabrera (1999), with C6 encompassing the Lagerstätte succession (Neumann and Cabrera, 1999; Storari et al., 2021a).

2.1.2 Solnhofen limestones

The Franconian Alb (Bavaria state) and Swabian Alb (Baden-Württemberg state) of Germany form a low mountain range extending from southwest to northeast in southern Germany and is composed of Lower to Upper Jurassic marine sedimentary rocks (Viohl, 2015) (Figure 1). Its fossil sites belong to five different formations, namely, Torleite, Geisental, Painten, Altmühltal, and Mörnsheim, from oldest to youngest, ranging from the late Kimmeridgian to the early Tithonian (Schweigert, 2015). These formations compose the Weißjura Group, a package of mainly calcareous marine sediments (Röper, 2005). Most fossils historically reported from these rocks come from the Altmühltal Formation (*sensu* Niebuhr and Pürner, 2014), however, fossils have also been recovered from the underlying Torleite and the overlying Mörnsheim formations (e.g., Tischlinger, 2001). They are often collectively called 'Solnhofen limestones', but the Solnhofen limestones *sensu stricto* are included only in the Altmühltal Formation and are restricted to the area northwest of the municipality of Ingolstadt, more commonly from areas of the municipalities of Solnhofen and Eichstätt, deposited during the Tithonian (Niebuhr and Pürner, 2014) (Figure 1). The Altmühltal Formation is biostratigraphically part of the Hybonotum Zone (Riedense and Rueppelianus subzones) (Barthel, 1978; Schweigert, 2007; Niebuhr and Pürner, 2014; Schweigert, 2015). To date, most insects were recovered from the areas around Eichstätt, and more rarely from the Solnhofen area or the rest of the Franconian Alb (Bechly, 2015). From now on, every time we mention the Solnhofen limestones in the text, we refer to the Solnhofen limestones *sensu stricto*, i.e., the Altmühltal Formation.

The Solnhofen limestones are divided into two types of rock, called Flinz and Fäule, that intercalate somehow cyclically (Munnecke et al., 2008). The fine-grained, hard limestone and

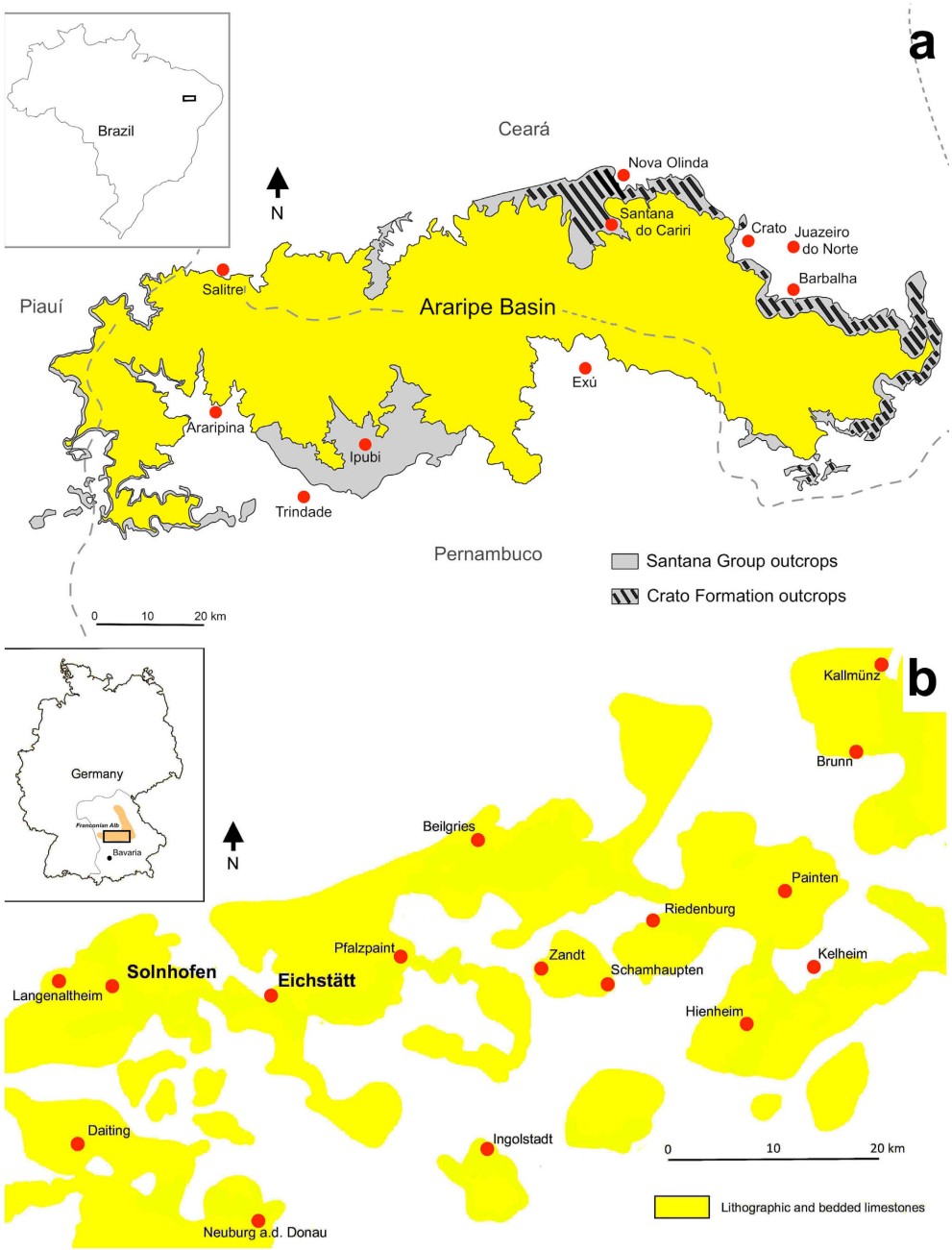

FIGURE 1
Crato Formation and Solnhofen limestones locality maps. **(A)** Locality map of the Araripe Basin and outcrops of the Santana Group and the Crato Formation within Brazil (modified from Storari et al., 2020; Lima et al., 2021). **(B)** Map of the southern Franconian Alb with localities of the Upper Kimmeridgian and Lower Tithonian limestones deposits from the Solnhofen Archipelago (modified after Röper and Rothgaenger, 1995; Hess et al., 1999; and Heyng et al., 2015).

putatively micritic Flinz beds show carbonate contents of more than 96% (Bausch et al., 1994; Bausch, 2004; Munnecke et al., 2008). They are intercalated by softer interlayers (Fäule) that present a foliaceous appearance and are slightly less rich in calcium carbonate (usually under 85%; Bausch, 2004). The Fäule beds are also laminated, although the laminae are thinner compared with the Flinz beds (Park and Fürsich, 2002).

All sedimentary models proposed for the Solnhofen limestones agree that they were deposited in individual marine basins at the northern margin of the Tethys Sea, with the depositional setting composed of relatively shallow waters isolated from the open ocean by coral reefs (Keupp, 1977; Viohl, 1990). It has been suggested that the water column of the depositional setting was stratified, with hypersaline bottom waters and an anoxic sea floor (Barthel, 1978; Barthel et al., 1990). According to the latest depositional model published, proposed by Viohl (2015), tropical storms led to episodic mixing of these hypersaline, anoxic bottom waters with the oxygenated surface waters, which caused the death of nektonic and planktonic organisms.

2.2 Material

2.2.1 Crato Formation

We analyzed a total of 234 fossils from the Crato Formation, being 222 fossil mayflies (192 larvae and 30 adults of Hexagenitidae: Ephemeroptera), and 12 Grylloidea (Ensifera: Orthoptera). The specimens analyzed are housed in the following Brazilian institutions: Museu de Paleontologia Plácido Cidade Nuvens, Universidade Regional do Cariri, Santana do Cariri (MPPCN); Paleontological collection of the Centro Acadêmico de Vitória, Universidade Federal de Pernambuco, Vitória de Santo Antão (CAV); Paleontological collection of the Universidade Regional do Cariri, Crato (LPU); Scientific Paleontological Collection of the Instituto de Geociências of the Universidade de São Paulo, São Paulo (GP) (Table 1).

From the 222 fossil mayflies, 124 unnumbered larval specimens were collected during controlled excavations at the Mine Antônio Finelon (S 07° 07' 22,5'' e W 39° 42' 01''), Nova Olinda, Ceará State, Brazil (Table 1). The orthopteran CAV 0012 was collected in 2009 during a field trip of biology students of the Centro Acadêmico de Vitória (Universidade Federal de Pernambuco) in a well-known limestone mine, Mina do Demar, on the road that connects Nova Olinda and Santana do Cariri municipalities, Ceará state. The LPU specimens lack exact locality information as they have been collected by mine workers and donated to that collection. The GP specimens also lack exact locality information because they were recovered by the Brazilian federal police during an operation against fossil smuggling. Although those specimens lack exact locality details, all of them were probably collected from upper portions of the FA-4 layer (*sensu* Varejão et al., 2021) or layer C6 (*sensu* Neumann and Cabrera, 1999) from the Lagerstätte portion of the Nova Olinda Member.

2.2.2 Solnhofen limestones

We analyzed 110 mayfly specimens from the Solnhofen limestones. Most German collections that house mayflies from the Solnhofen limestones were visited to reduce bias in data collection, including already published material. The following institutions were visited: Bayerische Staatssammlung für Paläontologie und historische Geologie, Munich (SNSB-BSPG); Bürgermeister-Müller-Museum, Solnhofen (BMMS); Jura Museum, Eichstätt (JME); Museum Bergér, Eichstätt (MB); Seckenberg Research Institute and Museum, Frankfurt (SMF); Staatliches Museum für Naturkunde, Karlsruhe (SMNK); and Staatliches Museum für Naturkunde, Stuttgart (SMNS).

The localities of the fossils analyzed here (when available) are quarries in Eichstätt, but most lack stratigraphic information. All the 20 fossils from the Bérger Museum come from a quarry in Blumenberg, Eichstätt (stratigraphically from the Riedense Subzone; *eigeltingense* Horizon, Schweigert, 2015) (Table 2). We infer that the analyzed specimens come from Flinz layers based on the characteristics of their limestone slabs (see Results section), but more precise stratigraphic placement is unavailable as original sampling information is lost. We analyzed only winged individuals since mayfly larvae were never reported for the Solnhofen limestones.

2.3 Methods

From the 234 Crato Formation fossils analyzed macroscopically, ten specimens were selected to be investigated in detail. The specimens were subjected to analytical analyses using scanning electron microscopy coupled to energy-dispersive X-ray spectroscopy (SEM-EDS), energy-dispersive X-ray fluorescence (EDXRF), and μRaman spectroscopy (six mayflies: MPSC I 763, MPSC I 2533, MPSC I 5224, MPSC I 5227, MPSC I 5229, MPSC I 5230; and three crickets: CAV 0012, LPU P6, GP1E 8910) (Table 1; Figure 2). From the 110 Solnhofen limestone fossils analyzed macroscopically, five specimens were also taken for SEM-EDS and μEDXRF analyses under the following inventory numbers: SMNS 70310; SMNS 70311a; SMNS 70311b; MB2021.10.155; MB2021.10.163; and MB2021.10.164a (Figure 3).

Micro morphological and elemental analyses of the fossils of the Crato Formation were conducted using a scanning electron microscope (SEM) FEI Quanta 250 with an Oxford Si(Li) energy-dispersive X-ray spectroscopy (EDS) detector coupled to the Oxford AZTec software at the Instituto de Geociências, Universidade de São Paulo, Brazil. Micro morphological and elemental analyses of the fossils of the Solnhofen limestones were conducted using a scanning electron microscope JEOL JSM-6500F equipped with an Oxford INCA Energy 200 EDS system with a crystal type 300 (energy resolution 133eV), at the Center for Light-Matter Interaction, Sensors & Analytics (LISA+), at the University of Tübingen, Germany. EDS point and mapping spectra were employed to highlight qualitative elemental heterogeneities in different regions (mostly due to topography differences, as specimens are presented as a flat surface with topographic irregularities), thus results obtained with EDS were considered in a qualitative approach only (Osés et al., 2016).

Energy-dispersive X-ray fluorescence (EDXRF) analyses were performed for rapid characterization of heavier and trace elements, to complement EDS measurements, since EDS detects light elements better (Pan et al., 2018). EDXRF analyses of the Crato Formation specimens were performed at the Instituto de Física, Universidade de São Paulo, Brazil. The portable equipment used consists of a mini Amptek X-ray tube of Ag anode and an Amptek fast Silicon Drift Detector (SDD) of 125 eV FWHM for the 5.9 keV line of Mn. Measurements were carried out with 30 kV voltage and 30 μA of tube current and with an excitation/detection time of 200 s (Barling et al., 2015; Osés et al., 2016, 2017). Data was processed in the softwares WinQxas, Spectragryph (Menges, 2022), Excel, and Inkscape. Solnhofen limestone specimens were analyzed with different equipment at the Mineralogical and Geochemical Micro-Analytical Laboratory (MAGMA Lab), Department of Applied Geochemistry, Technische Universität Berlin, Germany. μEDXRF analyses were made using the "area" mode of a Bruker Tornado M4 micro-XRF. Acceleration voltage was 50 kV using a beam current of 600 μA. Since Solnhofen fossils were more challenging to analyze, after several tests with specimens, we chose to work with a higher voltage. The measuring point distance was 20μm at 20μm beam diameter. The measuring time was 30 ms per analysis spot. To obtain more precise data from a stronger signal, the analyses were run with two simultaneously operating spectrometers.

10.3389/fevo.2024.1445160

TABLE 1 Specimens from the Crato Formation analyzed.

Identification	Ontogeny	Locality	Specimen(s)	Reference
Araripegryllus cf. *femininus*	Adult	Mina do Demar, Nova Olinda	CAV 0012	Analyzed in person at LPU
Cearagryllus sp. *indet*	Adult	n/a	LPU P6	Analyzed in person at LPU
Costalimella zucchii	Adult	n/a	LP/UFC CRT 1276 (holotype)	Brandão et al. (2021)
Cratohexagenites longicercus	Adult	n/a	MSF O46	Staniczek (2007)
Cratohexagenites longicercus	Larva	n/a	MURJ 447 (holotype)	Staniczek (2007)
Cratohexagenites minor	Larva	n/a	MB.I.2026 (holotype)	Staniczek (2007)
Gryllidae *indet.*	Adult	n/a	LPU P2	Analyzed in person at LPU
Grylloidea *indet.*	Adult	n/a	GP1E 7268; GP1E 7409; GP1E 8691; GP1E 8827; GP1E 8910; LPU 1196; LPU P1; LPU P3; LPU P4	Analyzed in person at the IG-USP and LPU
Hexagenitidae *incertae sedis*	Adult	n/a	LPU 1144, MPPCN I 763, MPPCN I 1559	Analyzed in person at the MPPCN
Protoligoneuria heloisae	Adult	n/a	AMNH 43499 (holotype)	Storari et al. (2021b)
Protoligoneuria limai	Adult	n/a	GP/1E 6763, GP/1E 6764, GP/1E 6766, GP/1E 6884, GP/1E 7221, GP/1E 8754, GP/1E 9034, GP/1E 9562, LPU 1696, MPPCN I 1559, MPPCN I 1631, MPPCN I 409, MPPCN I 4286cp, MPPCN I 4286p, MPPCN I 4287, MPPCN I 4313, MPPCN I 4422, MPPCN I 456, MPPCN I 469, MPPCN I 472	Analyzed in person at the IG-USP, and MPPCN
Protoligoneuria limai	Adult	n/a	RGMN T002, RGMN T004, RGMN T005, SMNS 66635, SMNS 70312	Martins-Neto (1996); Staniczek (2007)
Protoligoneuria limai	Larva	Mina Antonio Finelon, Nova Olinda	124 unnumbered specimens	Analyzed in person at the MPPCN
Protoligoneuria limai	Larva	n/a	AMNH 43404, AMNH 43415, AMNH 43418, AMNH 43435, AMNH 43452, AMNH 43455, AMNH 43469, DGM 6255, DGM 6256, DGM 6277, LPRP/USP 0583, RGMN T001, RGMN T003, RGMN T006, SMNS 66537	Brito (1987); McCafferty (1990); Martins-Neto (1996); Staniczek (2007); Brandão et al. (2021)
Protoligoneuria limai	Larva	n/a	GP/1T 2583, LPU 1141a, LPU 1141b, LPU 1647, LPU 1698, LPU-EC03, MPPCN I 1336, MPPCN I 1354, MPPCN I 1368, MPPCN I 1439, MPPCN I 2309, MPPCN I 2503, MPPCN I 2504, MPPCN I 2505, MPPCN I 2506, MPPCN I 2507, MPPCN I 2508, MPPCN I 2509, MPPCN I 2510, MPPCN I 2511, MPPCN I 2512, MPPCN I 2513, MPPCN I 2514, MPPCN I 2515, MPPCN I 2516, MPPCN I 2519, MPPCN I 2521, MPPCN I 2522, MPPCN I 2524, MPPCN I 2525, MPPCN I 2526, MPPCN I 2528, MPPCN I 2529, MPPCN I 253, MPPCN I 2531, MPPCN I 2532, MPPCN I 2533, MPPCN I 2536, MPPCN I 2537, MPPCN I 289, MPPCN I 293, MPPCN I 300, MPPCN I 301, MPPCN I 310, MPPCN I 770, MPPCN I 946, MPPCN I 5227, MPPCN I 5229, MPPCN I 5230	Analyzed in person at the IG-USP, and MPPCN

'n/a' means that the exact locality of the specimen sampling within the Crato Formation is unknown. Gray cells represent the orthopteran specimens studied.

10.3389/fevo.2024.1445160

TABLE 2 Winged mayfly specimens from the Solnhofen limestones biostratinomically analyzed and their available locality information.

Identification	Locality	Specimen(s)
Ephemeroptera *incertae sedis*	Eichstätt	JME 1748, JME 4675, JME 2054, JME 3668a, JME 3668b
Ephemeroptera *incertae sedis*	n/a	JME 1747, JME 3703a, JME 3703b, SMNK 2123, SMNK 2850, SMNK 2851, SMNK-PAL 45775
Hexagenites cellulosus	Eichstätt	BSPG AS I 748 (holotype)
Hexagenites sp.	Eichstätt	SMNS 70310
Hexagenites sp.	Eichstätt, Blumenberg quarry of the Bérger family	MB2021.10.151, MB2021.10.152a, MB2021.10.152b, MB2021.10.153, MB2021.10.154, MB2021.10.155, MB2021.10.156, MB2021.10.157a, MB2021.10.157b, MB2021.10.158, MB2021.10.159, MB2021.10.160, MB2021.10.161, MB2021.10.162, MB2021.10.163, MB2021.10.164a, MB2021.10.164b, MB2021.10.165, MB2021.10.166
Hexagenites sp.	n/a	BMMS 369, BMMS 53/72a, BMMS 53/72b, BMMS A, BMMS B, BMMS 2020, JME 2327, SMF VI 1362, SMNS 70311A, SMNS 70311B
Hexagenites multinervosa	n/a	BSPG 1964 XXIII 589 a, BSPG 1964 XXIII 589 b
Mesephemera procera	Eichstätt	BSPG AS I 1027 (holotype), JME 1728, JME 1736a, JME 1736b, JME 1738, JME 1742, JME 1743, JME 3691a, JME 3691b, JME 4672
Mesephemera procera	n/a	BSPG 1964 XXIII 3a, BSPG 1964 XXIII 3b
Mesephemera lithophila	Eichstätt	BSPG AS VII 497 (holotype)
Mesephemera speciosa	Eichstätt	BSPG 1882 XVI 30 (holotype), BSPG AS I 808, BSPG AS I 809, JME 1745
Mesephemera sp.	Eichstätt	BSPG 1965 III 20, JME 4673, JME 4674
Mesephemera sp.	n/a	BSPG 55229
Mesephemera? prisca	Eichstätt	BSPG AS V 37
Olgisca mortua	Eichstätt	JME 1744
Olgisca schwertschlageri	n/a	JME 1746
Pedephemera multinervosa	Eichstätt	BSPG 1961 III 54
Pedephemera multinervosa	n/a	BSPG 1961 I 467a, BSPG 1961 I 467b, BSPG 1964 XXIII 1, BSPG 1964 XXIII 2a, BSPG 1964 XXIII 2b, BSPG 1964 XXIII 3, BSPG 1972 XX 12, BSPG 1972 XX 13
Paedephemera schwertschlageri	Eichstätt	JME 1750a, JME 1750b, JME 1756
Paedephemera speciosa	Eichstätt	JME 2056
Paedephemera sp.	n/a	BSPG 1964 XXIIIa, BSPG 1964 XXIIIb

The mineralogical composition of the Crato Formation fossils was analyzed by Raman spectroscopy at the Instituto de Química, Universidade de São Paulo, Brazil, using a micro-Raman inVia Renishaw, coupled to a confocal light microscope. The excitation laser used for the measurements was of 785 nm wavelength. It used a x50 lens, 10s and 20s of exposure time, laser power of 1% and 5%, and 5-40 accumulations. The calibration was performed with the Si band at 520.7 cm-1 (ASTM International, 2002). The data processing of the Raman spectra was made using the softwares Spectragryph (Menges, 2022) and Inkscape. The obtained spectra were identified by comparison to the RRUFF project database (Lafuente et al., 2015).

3 Results

3.1 Crato Formation

3.1.1 Exceptional preservation of the Crato Formation insects

All the 124 mayfly specimens recovered from controlled excavations are preserved in yellowish limestones, with the fossils themselves displaying orange/rusty coloration (e.g., Figure 2). From those, the majority are preserved by replication (substitution) of the cuticle and tissues (86%; n=107), and only 14% of specimens are preserved as imprints (n=17).

SEM imaging of selected specimens reveals the preservation of fine details not discernible by the naked eye. External features include different microtextures of body segments (mayflies and crickets - specimens MPSC I 5227, MPSC I 5230, GP1E 8910), setation (mayflies - MPSC I 5227, MPSC I 5230), spines (mayflies - MPSC I 5227, MPSC I 5230), and spiracles (mayflies and crickets - MPSC I 5227, MPSC I 5230, GP1E 8910, LPU P6) (Figure 4). The observed internal features are interpreted as muscle fibers (mayfly MPSC I 5227), parts of larval mouthparts (mayfly MPSC I 5230), and parts of the inner gut, such as proventriculus (crickets - CAV 0012, GP1E 8910, LPU P6) (see also Storari et al., 2024) and crop (cricket specimen LPU P6) (Figure 4); as well as putative tracheal channels, and the morphology of gills (mayfly MPSC I 5227) (Figure 5A).

We also observed wrinkle-like texture of the cuticle (Figure 5A). There is a clear differentiation between the fossil and its matrix (Figure 5B), as they are replicas of the original organisms. We also visualized a superficial thin film at some parts of the well-preserved tissues of some fossils (only in the SEM secondary mode – Figures 5C, D) that we interpret as an extracellular polymeric substance (EPS) of biofilm, a mineralized (due to its carbon composition and morphology) coating over the fossil, obscuring the fabrics below (Barling et al., 2020), which in this case are scattered anhedral to subhedral crystals between rhombohedral crystals infilling cavities. While secondary electrons emit from a few nm in depth, backscattered electrons originate deeper in the sample, thus accounting for imaging of the calcite crystals underneath the shallow film. Some authors also call this surface, which occurs consistently along the specimen body, 'amorphous

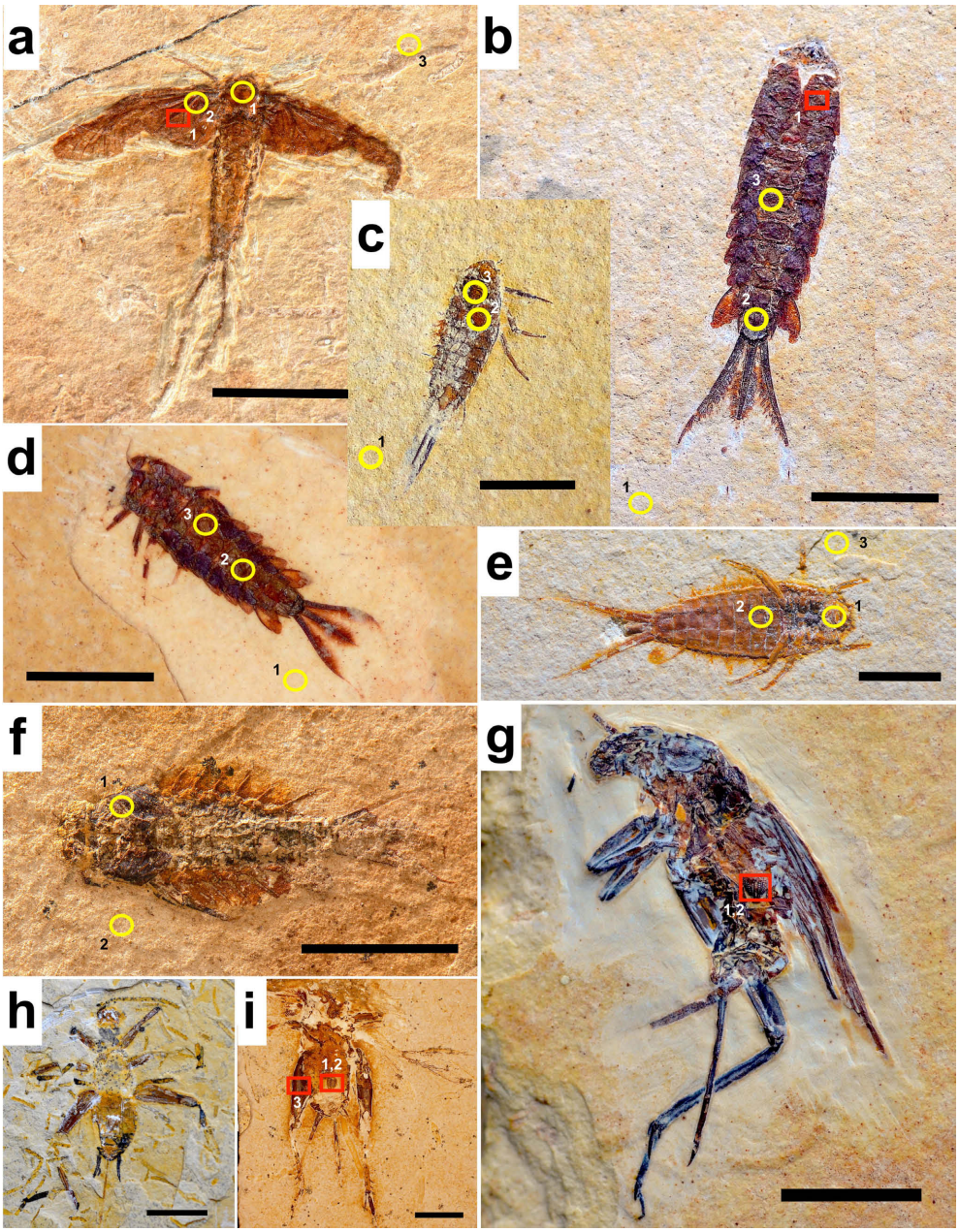

FIGURE 2
Crato insects examined under analytical techniques. Yellow circles refer to the locality of EDXRF points analyzed shown in Figures 11; Supplementary Figure B. Red rectangles refer to the locality of the points analyzed under Raman spectroscopy shown in Figure 10; Supplementary Figure D. **(A)** Winged Hexagenitidae mayfly MPSC I 763. Scale bar 10 mm. **(B)** Larval *Protoligoneuria limai* MPSC I 5229. Scale bar 5 mm. **(C)** Larval *P. limai* MPSC I 5224. Scale bar 5 mm. **(D)** Larval *P. limai* MPSC I 5227. Point 3 = P13 of Figure 11. Scale bar 5 mm. **(E)** Larval *P. limai* MPSC I 5230. Point 1 = P14 of Figure 11. Scale bar 5 mm. **(F)** Larval *P. limai* MPSC I 2533. Scale bar 5 mm. **(G)** Adult *Araripegryllus femininus* CAV 0012. Scale bar 5 mm. **(H)** Adult *Cearagryllus* LPU P6. Scale bar 10 mm. **(I)** Adult Grylloidea GP1E 8910. Scale bar 5 mm.

material', however, in some cases, it is only a thin layer (as seen here), and under which there is a carbonate matrix with abundant euhedral to subhedral calcite crystallites (Barling et al., 2020; Dias and Carvalho, 2020).

3.1.2 Microfabrics of external cuticle and internal tissues

SEM analysis revealed that the exceptionally well-preserved parts of fossils are, often, preserved by sub-spherical to spherical closely-packed grains, which we identify here as pyrite framboids or pseudoframboids (Figures 6A, B, 7, based on elemental composition and morphology of grains - following Grimes et al., 2002; Barling et al., 2015; Osés et al., 2016). The size of the framboids differs between the external cuticle and internal tissues (Figures 6E, F), with the external cuticle ones presenting diameters in the range of 5.0–10.0 μm, while in inner tissues they range from 0.4 to 1.0 μm. There is a clear differentiation among the microfabrics of the external cuticle and of the internal organs: large framboids compose the external cuticle

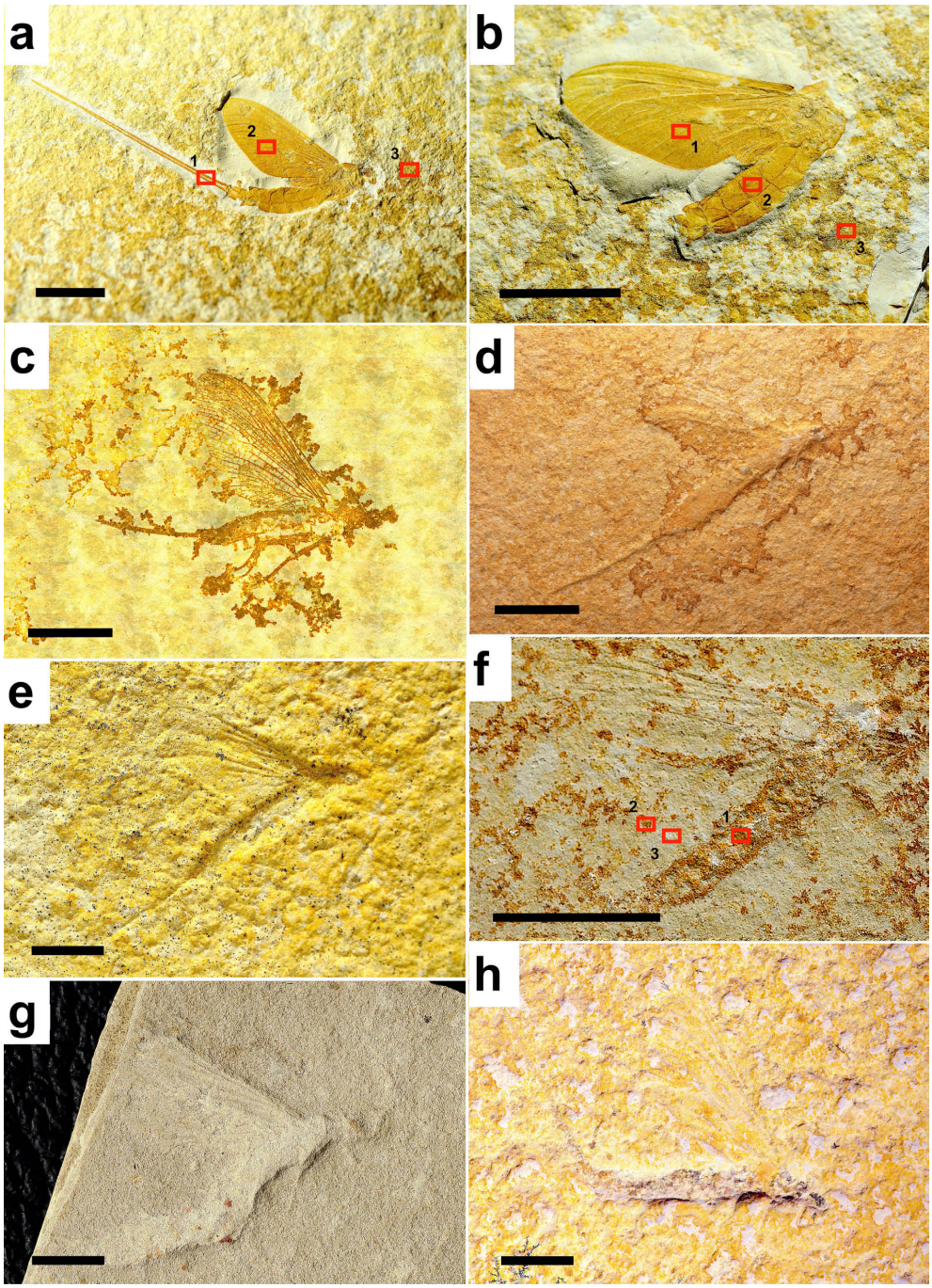

FIGURE 3
Solnhofen mayflies examined under analytical and biostratinomic analyses. **(A)** *Hexagenites* SMNS 70311a; **(B)** *Hexagenites* SMNS 70311b; **(C)** *Hexagenites* SMNS 70310; **(D)** *Hexagenites* BMMS 369; **(E)** *Paedephemera* SNSB 1964 XXIII; **(F)** *Hexagenites* MB2021.10.155; **(G)** *Hexagenites* SMF VI 1362; **(H)** Ephemeroptera *indet.* JME 2054. Scale bars 10 mm. Red rectangles refer to the locality of the EDS point spectra shown in Supplementary Figure D.

(Figures 6A, B) (as already illustrated by Osés et al., 2016; Barling et al., 2020; Bezerra et al., 2020; Dias and Carvalho, 2020), while the more rarely preserved inner organs (e.g., proventriculus) are formed by much smaller and more packed framboids; Figures 6E, F illustrate how the crystals are visible only between 4.000–8.000x magnification in the inner tissue, while in the cuticle they are visible in a smaller magnification. We additionally observed, associated with the well-preserved inner tissues, a cemented agglutinated mass (or amorphous matter as referred by Dias and Carvalho, 2022), probably related to EPS, following recent interpretations of Dias and Carvalho (2022) (Figures 6C–E).

We also notice a gradient pattern in the external cuticle. The parts with the best morphological fidelity consist of closely-packed and not framboid-shape (less circular) crystals, arranged like a scale;

10.3389/fevo.2024.1445160

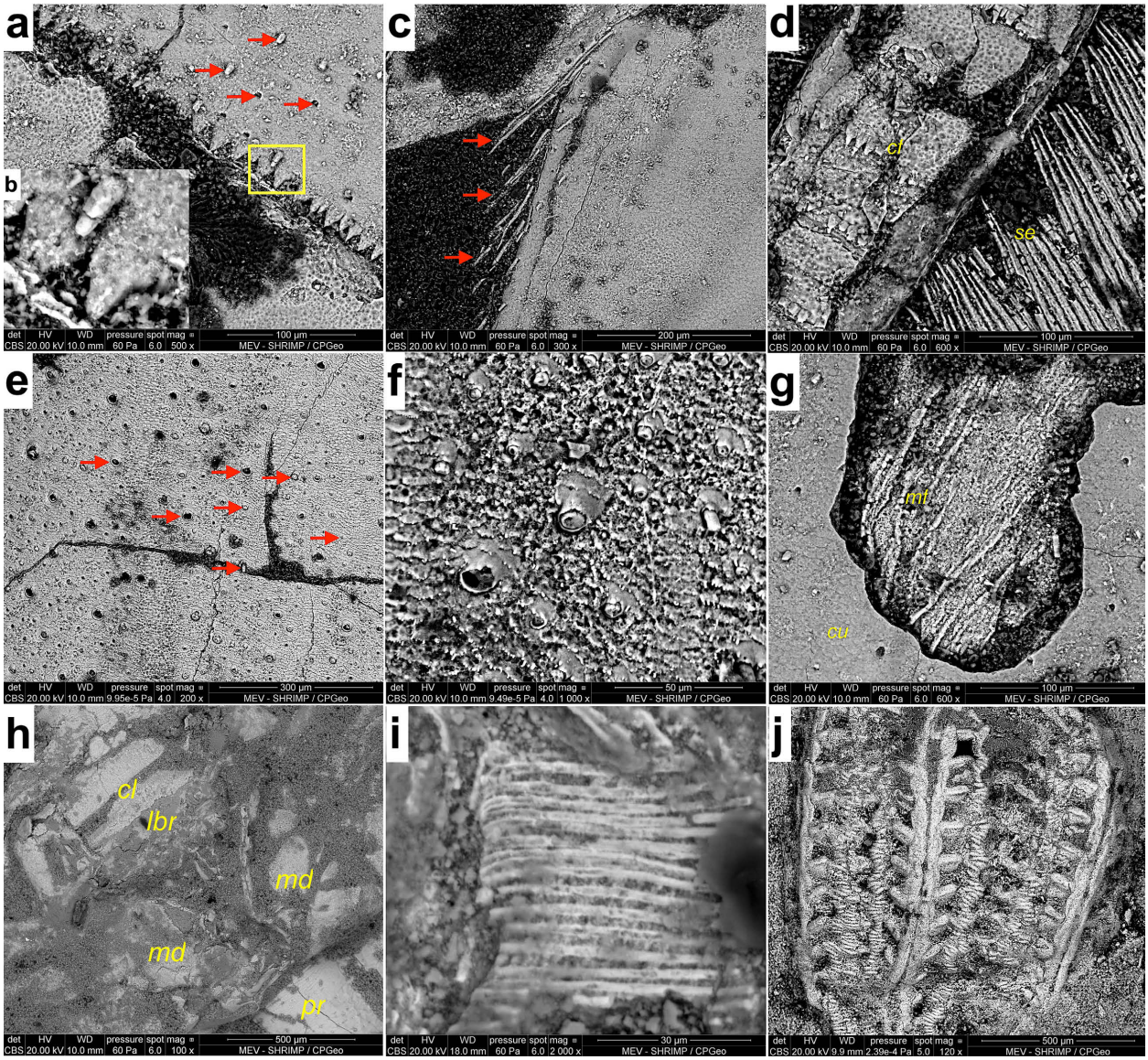

FIGURE 4
Exceptional preservation of morphological structures from the Crato Formation mayfly larva and crickets. **(A)** Microtexture of the cuticle and serrated border of abdominal segments of specimen MPSC I 5227 (*Protoligoneuria limai* larva); arrows point to spiracles as well as delicate setae. **(B)** Detail at higher magnification of delicate seta base delimited by the rectangle in 'a'. **(C)** Setation on the last abdominal segments of the larva MPSC I 5230 (*P. limai*). **(D)** Microtexture of the cuticle and serrated border of caudal filaments [cf] of the specimen in c; extensive setation [se] of caudal filaments laterally. **(E)** Scale-like texture of cuticle from specimen GP1E 8910 (Grylloidea) showing several spiracles as well as base of sensilla (arrows). **(F)** Detail of structures from 'e'. **(G)** Internal muscle fibers [mf] evidenced after cracking of outer cuticle [cu] at the last segment of the abdomen of the mayfly larva MPSC I 5227. **(H)** Mouthparts of larval mayfly specimen MPSC I 5230; cl - clypeus; lbr labrum; md - mandible; pr - prosternum. **(I)** Muscle fibers in the inner gut of *Araripegryllus* specimen CAV 0012. **(J)** Proventriculus of Grylloidea specimen GP1E 8910.

and the less preserved the surface is, the more dispersed and rounded-framboid-like the crystals are (Figure 7), as well-portrayed in the literature (Barling et al., 2015; Osés et al., 2016; Barling et al., 2020; Bezerra et al., 2020; Dias and Carvalho, 2020).

3.1.3 Elemental characterization of the Crato Formation fossils

EDS and EDXRF elemental mapping of the Ephemeroptera specimens revealed a marked preferential distribution of iron (Fe), oxygen (O), copper (Cu), zinc (Zn), and lead (Pb) in the fossil, and of calcium (Ca) in the host rock (Figure 8; Supplementary Figure A).

In the orthopteran fossils, EDS point analyses of the proventriculi show mainly Ca, phosphorous (P), and O occurring associated with the coatings of anhedral to euhedral crystals, and mainly Ca, P, O, Fe, and silicon (Si) at the film-embedding crystals (Figure 6B), though Ca and P counts are lower than those of the Ca/P-rich coating. Peaks of Ca and P are present in several parts of proventriculi and indicate preservation by calcium phosphate (Figure 9).

In the EDS maps of the proventriculi of specimens CAV 0012 and LPU P6 (Figure 8), we also observe sulfur (S) associated with Fe in some areas. Zn is associated with Fe in the fossil. As observed in

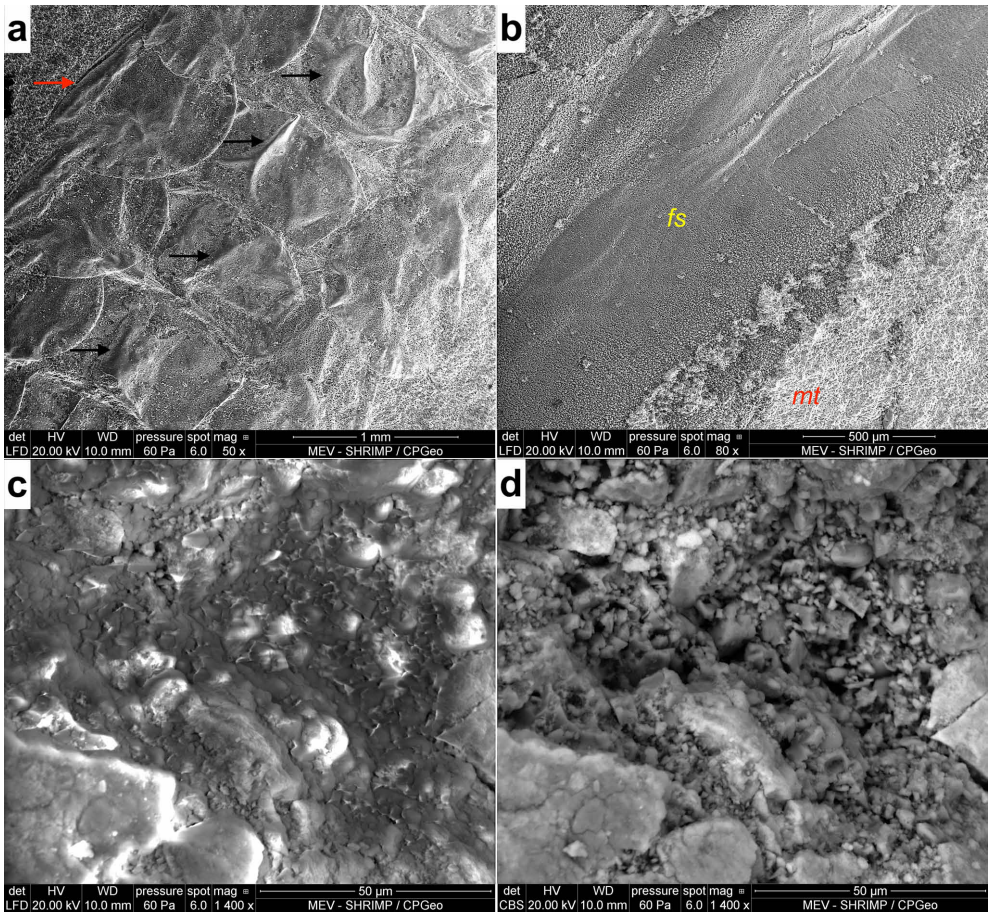

FIGURE 5
External structural features of preservation in mayfly larvae and orthopterans of the Crato Formation. **(A)** larval *Protoligoneuria limai*, specimen MPSC I 5227 preserving wrinkle-like external texture of the cuticle in the abdominal terga (wrinkles indicated by black arrows); laterally the border of thin layer of gills and hard costal rib (red arrow) are also visible. **(B)** Clear differentiation between fossil [fs] and matrix [mt], grylloid specimen LPU P6 (*Cearagryllus*). **(C)** Superficial film preserved at mouthparts of the mayfly larva MPSC I 5230 (*P. limai*). **(D)** The same area of Figure 'c' showing scattered anhedral to subhedral crystals between rhombohedral crystals, underneath the film in 'c', which usually infill body cavities in the specimens analyzed.

the EDS spectra, maps show the spatial correlation of Ca and P at the proventriculi coating.

In EDS point spectra of the proventriculus of specimen GP/1E 8910, the main elements are Ca, S, and O, followed by Fe and Si, while in some cases, Fe peaked more expressively than these latter elements (Supplementary Figure B). The inner gut tissue also has high counts, mainly of Si and O at the well-preserved denticle-like surface (Figure 10B). Finally, peaks of manganese (Mn) were recovered around the well-preserved inner gut, associated with peaks of both Ca and Fe (Supplementary Figure B).

EDXRF analyses of Ephemeroptera larvae show that the fossils are composed of Ca, Cu, Zn, Fe, Si, S, potassium (K), titanium (Ti), chromium (Cr), Mn, strontium (Sr), Pb, S, and chlorine (Cl) (Figure 10; Supplementary Figure C). The main element of the host rock is Ca, but it also has negligible counts of S, Cl, and Ti (Figure 10; Supplementary Figure C). Si, Ca, K, Sr, Pb, and Mn are more abundant in the host rock, while the other elements do not show a clear correlation with either the host rock or the fossils, or are more significant in the latter (Figure 10B). The relative intensities of Ca and of Sr seem to be correlated, with more counts of these elements in the host rock (Figure 10B). When only a single fossil is considered, the relative intensities of some metals vary among different measurement points. For instance, in specimen MPSC I 763, Ti, Cr, Fe, Cu, Zn, and Pb have lower counts in P14 relative to P13 (Figure 10B).

Micro-Raman results are similar to the EDS results and indicate that iron oxides/hydroxides, particularly goethite, preserve the biological tissues of specimens. Strong bands defining goethite are 295 and 393 cm^{-1} (Perardi et al., 2000; Li and Hihara, 2015), and in our fossils, Raman spectra also have bands at ca. 300 and 395 cm^{-1} (Figure 10). Calcite was also found to be represented by a strong band in 1086 cm^{-1} (Figures 10C, E).

3.2 Solnhofen limestones

3.2.1 Preservation of mayflies from Solnhofen limestones

Almost all the specimens are fossilized in lateral position (n=82), except two isolated wings (BMMS 53/72a and BMMS 53/72b), and specimen BSPG 4672 preserved either in dorsal or ventral

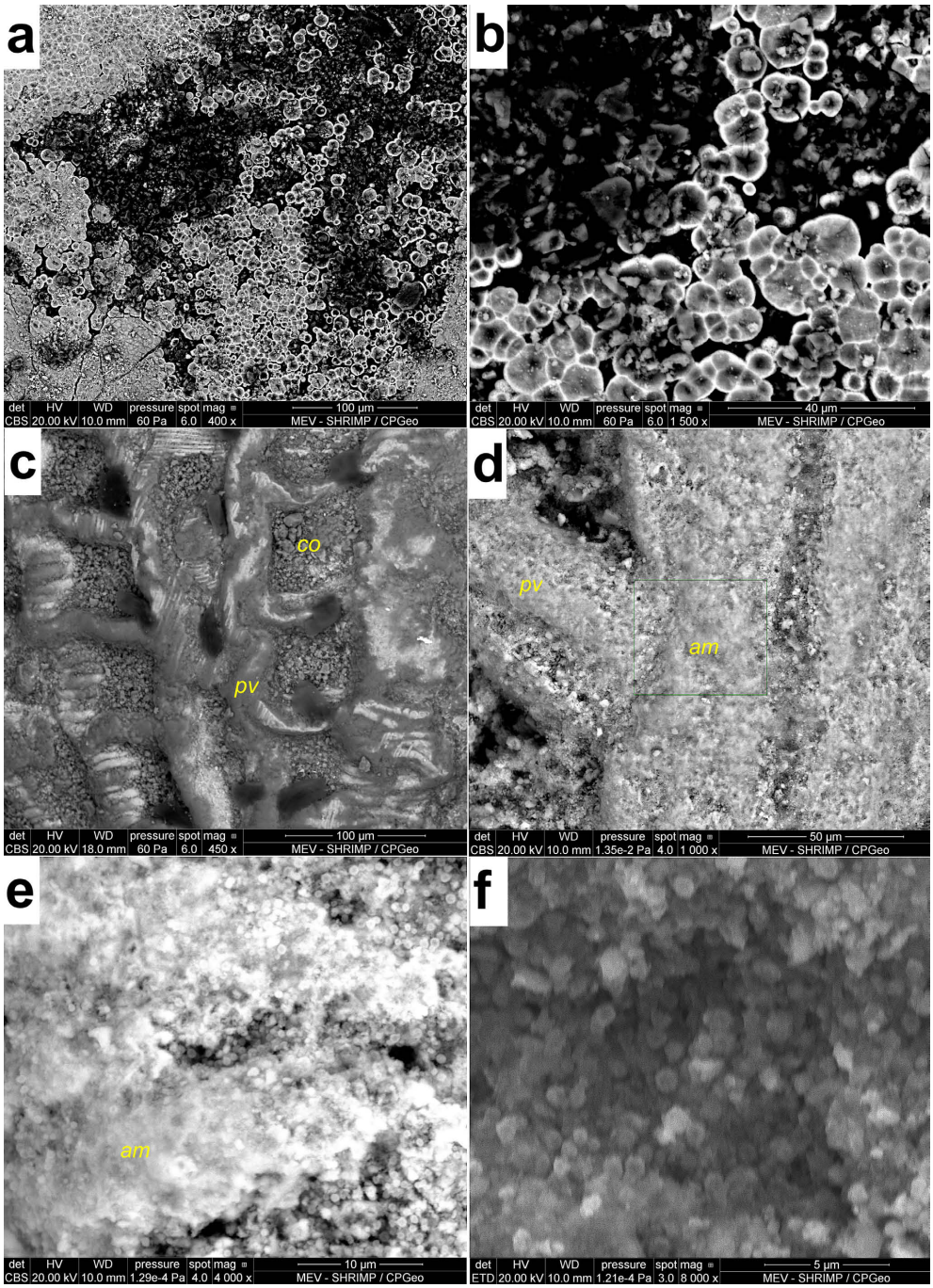

FIGURE 6
Microfabrics of external cuticle and internal tissues from insects of the Crato Formation. **(A, B)** Pseudoframboids from external cuticle in different magnifications. **(C–F)** Parts of proventriculi under different magnifications. **(C)** Coating [co] of proventriculus with a random coarse mix of disorganized anhedral and euhedral crystals, together with the 3D well-preserved part of the proventriculus [pv]. **(D)** A close-up of [pv] from figure 'c' showing the external microfabric texture of the proventriculus. **(E)** Microfabric of 3D well-preserved proventriculus showing the aggregate of microframboids immerse in a mass [am] of unstructured form. **(F)** Close-up of figure 'e' showing sub-spherical to spherical microframboids.

position (preservation is so low that is not discernible). Also, almost half of the specimens are complete (n=38), considering the main body parts (head, thorax, abdomen, and caudal filaments). All fossils studied show a low degree of morphological fidelity, with body segments indistinguishable in most of the cases (e.g., lines that mark where is the end of the thorax and beginning of the abdomen; lines delimiting abdominal segments – Figures 3D–H).

Solnhofen mayflies are preserved only as faded imprints in the limestone slabs (Figure 3). The only exceptions are the specimens SMNS 70311a and b (the slab and counterslab of the same

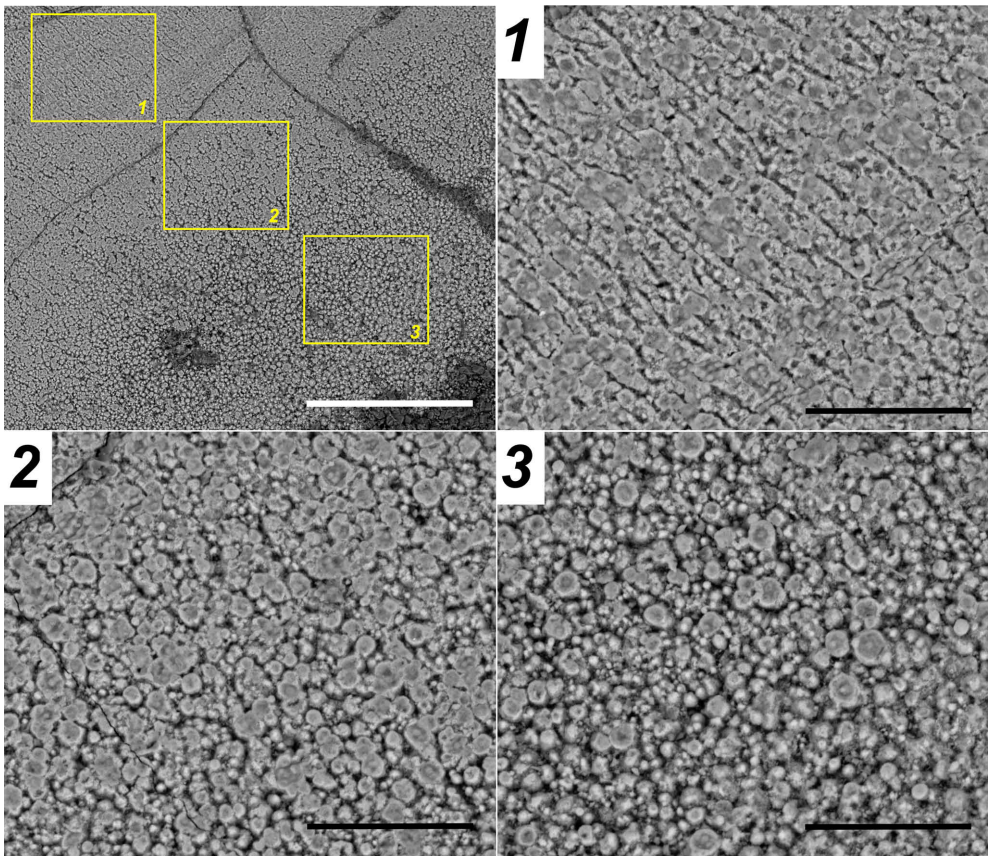

FIGURE 7
External cuticle gradient pattern from insects of the Crato Formation. External cuticle of the grylloid LPU P6 showing a gradient pattern related to the preservation of the cuticle. In the more preserved areas [1], the crystals are less spherical in shape, and are more scale-like and long, in a closely-packed arrangement. [2] shows an intermediate area and [3], a less well-preserved area. Images were recovered using the backscattered detector; magnifications are 250x in the first photo and 1000x in the subsequent ones; scale bars 200μm in the first photo and 50μm in the subsequent ones; spot size 6.0; working distance (WD) of 10 mm.

individual), which are preserved by a mineral film covering their imprints (visually similar to a mineral replacement), and are the only macroscopically well-preserved specimens (Figures 3A, B).

SEM imaging revealed that the preservation of the external morphology of the fossils is very low, and internal preservation is non-existent, with tissues obliterated by calcite crystals or in combination with globular material (possibly crystals of iron oxi/hydroxides) (Figure 11). Half of the specimens (n=43) present calcite crystals associated with and obliterating body parts, especially the eyes (Figures 3A, D, F, H). Only seven specimens present their abdominal segments delimited, although weakly (Figures 3E, G, H). Also, in a few cases (specimens BSPG 1882 XVI 30, JME 1728, JME 1745, JME 3703a/b, and SMNS 70311), the wing venation and/or body was traced by iron oxide dendrites in combination with ferrous solutions in a disorganized way (Figures 3C, D - see elemental results below).

3.2.2 Elemental characterization of the mayflies from Solnhofen limestones

EDS point analyses of mineral fabrics revealed similar chemical concentrations when comparing the fossil and the matrix, with a marked preferential concentration of Ca, with only slight differences. Although abundant Ca can also indicate the presence of aragonite, the fossils we analyzed here are clearly dominated by calcite, recognized due to the distinct orthorhombic shape of their crystals (see Figure 11; Bragg, 1924).

The typical pattern among all areas we analyzed is that Ca is the most abundant element, followed by O and carbon (C), except the matrix of specimen MB2021.10.155 in which Ca was most abundant, followed by Si, then aluminum (Al) (Supplementary Figure E). Phosphorus was noted in only one sampled point of the abdomen of specimen MB2021.10.155. Sulfur was also only recovered in small amounts in specimen MB2021.10.155 (both fossil and matrix).

Generally, apart from Ca, O, and C as the most abundant elements, in most analyzed areas, Si stands out, together with Fe, S, magnesium (Mg), Al, K, barium (Ba), and Mn. Fe, Al, Mg, and Ba are found frequently, while S, K, and Mn are recovered occasionally (Supplementary Figure E).

Elemental analyses revealed that Fe is more concentrated in fossils than in the rock matrix, while Ca is slightly more concentrated in the rock, although overall signals are very similar. The preferential distribution of these elements is consistent with Fe compounds replacing the fossils and the calcitic composition of the rock matrix.

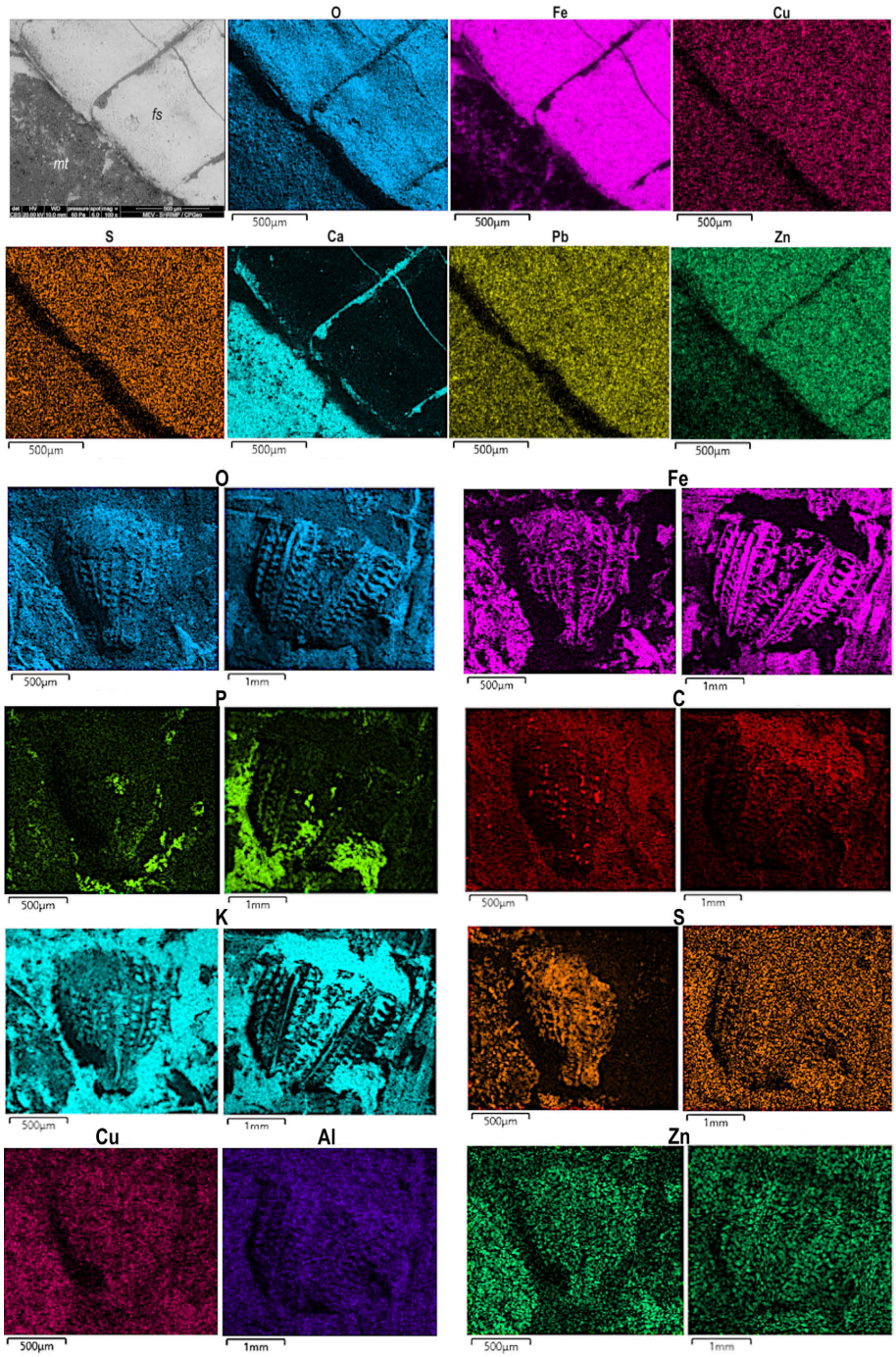

FIGURE 8
Elemental mapping of mayfly larva and proventriculi of orthopterans. The first two rows of images are the abdominal segments of *Protoligoneuria limai*, specimen MPSC I 5230. fs - fossil, mt - matrix. Below are the mapping of orthopteran proventriculi from specimens CAV 0012 (left) and LPU P6 (right). Images were recovered using the backscattered detector, with spot size 6.0. CAV 0012 - magnification 80x, WD 18 mm. LPU P6 - magnification 40x, WD 10 mm. O - oxygen, Fe - iron, P - phosphorus, C - carbon, Ca - calcium, S - sulfur, Cu - copper, Al - aluminum, Zn - zinc, Pb - lead.

Microenergy-dispersive X-ray fluorescence analyses (µEDXRF) agree with EDS, recovering Ca and O as the more prominent elements in all the specimens (Figure 12). Iron is relatively well represented but not as much as O. The remaining elements occurring in fossils are Mg, Sr, S, Mn, Ti, Zn, and Cu (Figure 12). Usually, better-preserved parts are those with high Fe content (Figures 12, 13); parts that are massively taken by calcite crystals, as the eyes of specimen SMNS 70311a, have no Fe and the elemental composition of these crystals is very similar to that of the calcitic matrix, with also almost no Fe at all. The calcite crystals obliterating the eyes, for instance, are also associated with metals such as Sr and Zn (Figure 13; Supplementary Figure F). In the only case in which

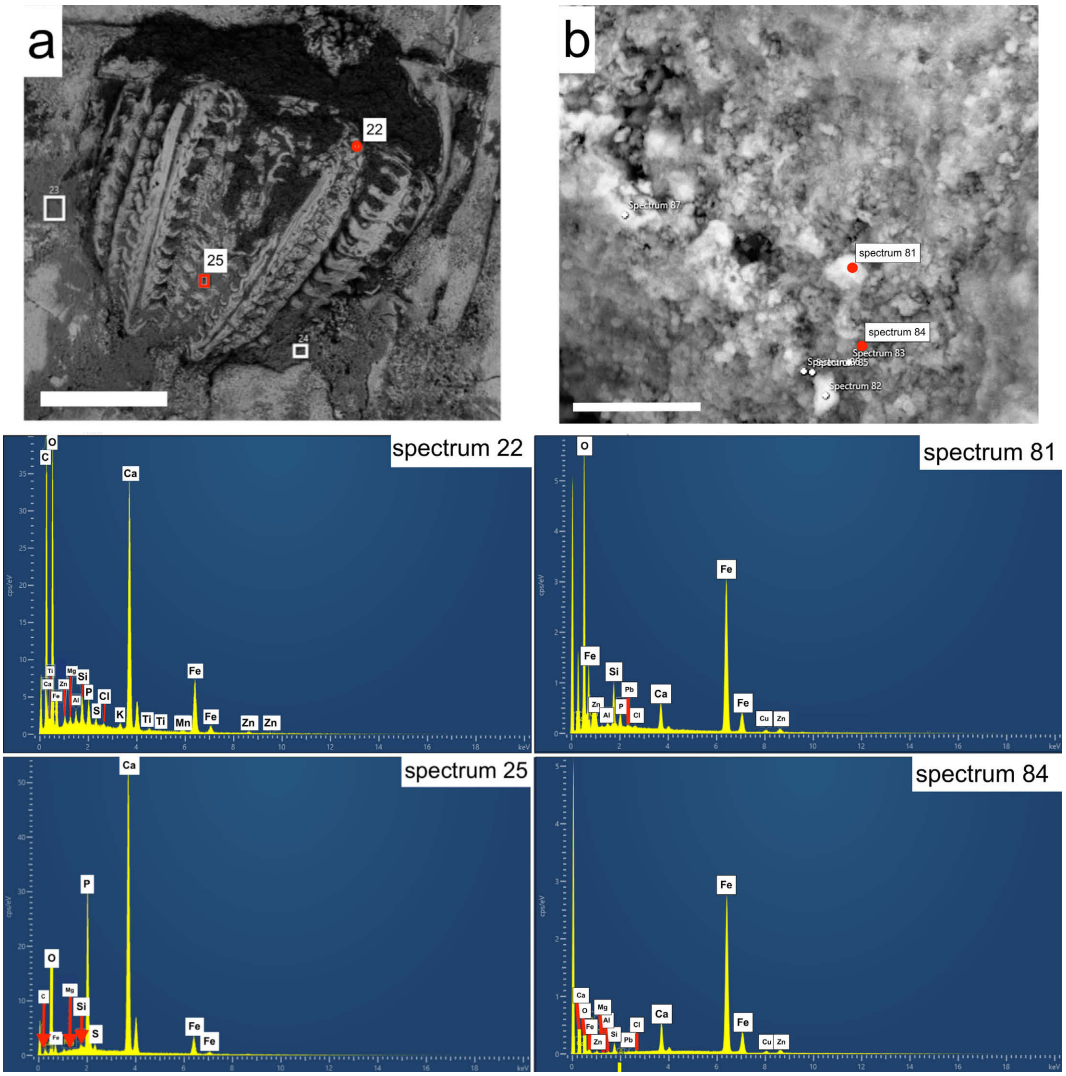

FIGURE 9
Energy-dispersive X-ray spectroscopy (EDS) point spectra of the proventriculus of the orthopterans. **(A)** Some point spectra of the proventriculus of specimen LPU P6. Scale bar 1 mm. **(B)** EPS-like superficial foam covering and infilling parts of proventriculus of specimen GP/1E 8910. Scale bar 10 μm.

the specimen is associated with iron/manganese oxide dendrites (SMNS 70310), we could identify that the Fe is in a combination with other metals such as Ti and Mn (Figure 13; Supplementary Figure G). Similarly, in the best-preserved specimen SMNS 70311a, Fe, Mn, Ti, and Zn occur preferentially in the fossil relative to the host rock (Figure 13; Supplementary Figure F).

4 Discussion

All the Crato fossils we analyzed in the present work were initially pyritized specimens that were secondarily replaced by iron oxides/hydroxides, as indicated by the brown, yellow, and orange-brown colors of the fossils (Figure 2) (Osés et al., 2016, 2017), and by Raman data. An original pyrite mineralogy is additionally supported by both the microfabric morphology of pseudoframboids and the elemental composition. The regions of high preservational fidelity, like the proventriculi, are replaced by pseudoframboids that are always smaller when compared to those of the cuticle. Barling et al. (2020) showed similar results, but they discussed that the high-fidelity fabric (i.e., smaller crystals) only replaces the epicuticle, whereas the pseudomorphic framboid (i.e., bigger crystals) replaces internal tissues and subsurface cuticular layers, which is the opposite of what we show here. Probably, the smaller close-packed grains are not necessarily related to inner or outer parts, but to the well-preserved ones. According to Briggs et al. (1993), the smaller the calcium phosphate particle aggregates are, the higher the morphological fidelity of preservation. A similar interpretation is supported for pyritization of Crato insects by Delgado et al. (2014); Osés et al. (2016), and Barling et al. (2020), suggesting that areas of high-fidelity cuticle replacement are a consequence of the close packing of the framboids.

Soft tissue phosphatization has been reported before in insects from the Crato Formation (Dias and Carvalho, 2020). In our

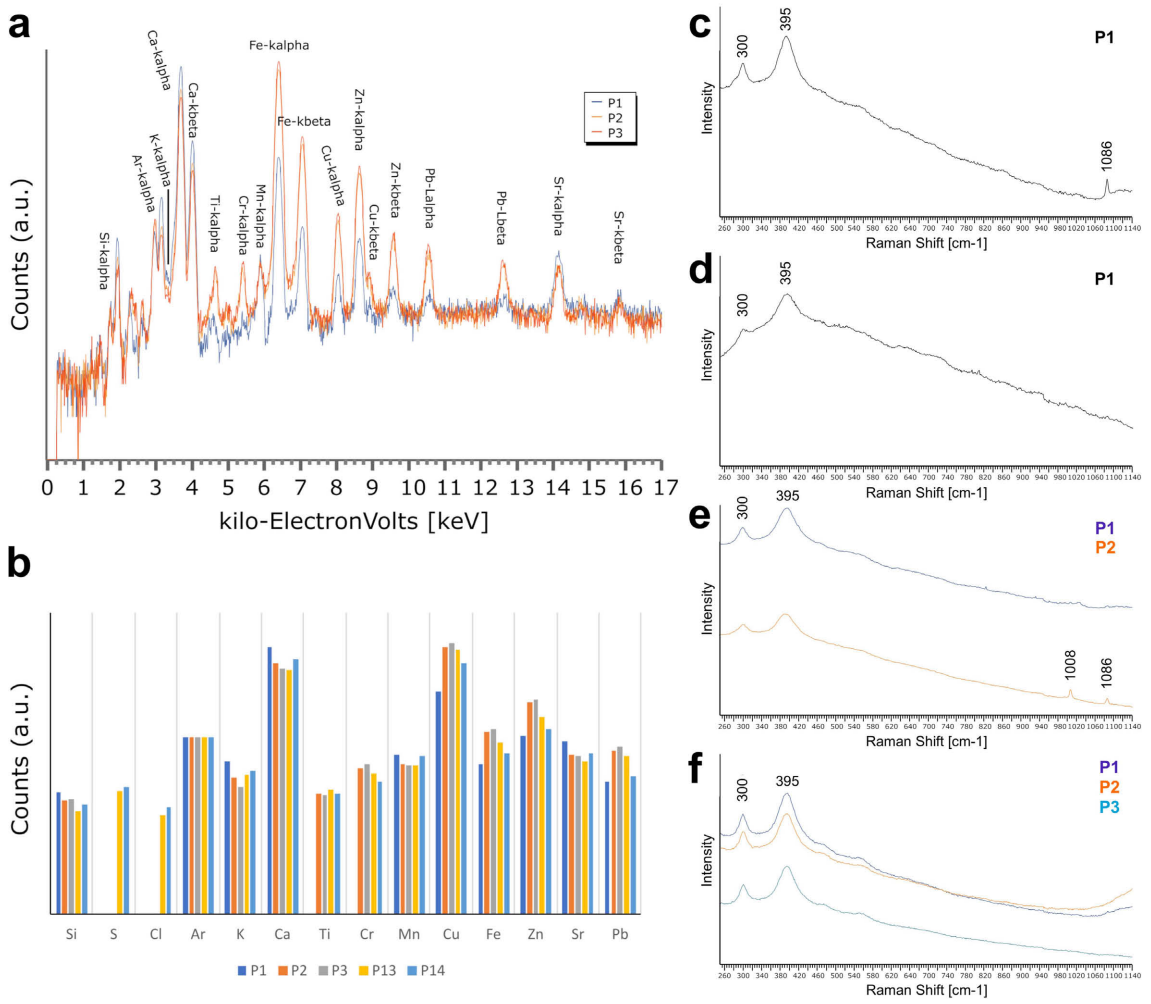

FIGURE 10
Energy-dispersive X-ray spectroscopy analyses and Raman spectra from Crato mayflies and crickets. **(A, B)** EDXRF analyses of Ephemeroptera larvae and host rock. **(A)** EDXRF point spectra measured in specimen MPSC I 5224. P1-Rock, P2-Fossil and P3-Fossil. b) Plot of relative intensities (log scale) for measured elements in different points of host rock and fossils (specimens MPSC I 5224 - P1,2,3; MPSC I 5227 - P13; and MPSC I 5230 - P14). P1-Host rock, P2-Fossil, P3-Fossil, P13-Fossil, and P14-Fossil. Points analyzed within specimens are marked in Figure 2. **(C–F)** Raman spectra from larval mayflies and adult orthopterans. c) Specimen MPSC I 763. **(D)** Specimen MPSC I 5229. **(E)** Specimen CAV 0012. **(F)** Specimen GP/1E 8910. Band of goethite (ca. 300 cm^{-1} and ca. 395 cm^{-1}) and of calcite (ca. 1086 cm^{-1}). Location of points analyzed in Figure 2, Supplementary Figure D.

observations, it is restricted to some areas of the orthopteran proventriculi and to regions surrounding them. EDXRF data indicates negligible amounts of sulfur in the host rock relative to the Crato mayfly fossils, and EDS maps of orthopteran proventriculi indicate that this element is not associated with iron. This may imply that sulfur in the Crato fossils occurs in other mineral phases, like sulfates, after sulfide oxidation (Osés et al., 2016). This is supported by low sulfur counts when iron is abundant and high counts of sulfur and calcium in some areas, which relates to the remaining iron sulfides of the primary pyritization process (Osés et al., 2016). We noticed that when only a single fossil is considered, the relative intensities of some metals vary among different measurement points (e.g. specimen MPSC I 763, Fe, Cu, Zn, and Pb have lower counts in P14 relative to P13 - Figures 2, 10). This observation may be related to the distinct preservation of the morphological structures in these two points, as P14 was measured in a wing and P13 in the head/thorax. Osés et al. (2016) hypothesized that these metals were originally associated with sulfides. It is possible that more readily available labile organic matter in the head/thorax region favored more decay and sulfide precipitation relative to the wings, thus explaining more abundance of these elements in the body.

Nevertheless, the preservation of Crato insects is diverse and includes further preservational pathways than those exemplified here (pyritization and phosphatization). For example, carcasses may also be kerogenized (see Barling et al., 2020; Bezerra et al., 2020; Dias and Carvalho, 2020, 2022). Pyritization and kerogenization are associated with different types of laminated limestones: pyritized specimens occur mainly in yellowish limestones, while kerogenized fossils are preserved in grayish limestones (Barling et al., 2020; Dias and Carvalho, 2022). As we report above, the dominant fabric of preservation of the pyritized fossils is goethite pseudomorphs of framboidal pyrite. In the kerogenized fossils, there is a massive carbonaceous film on the

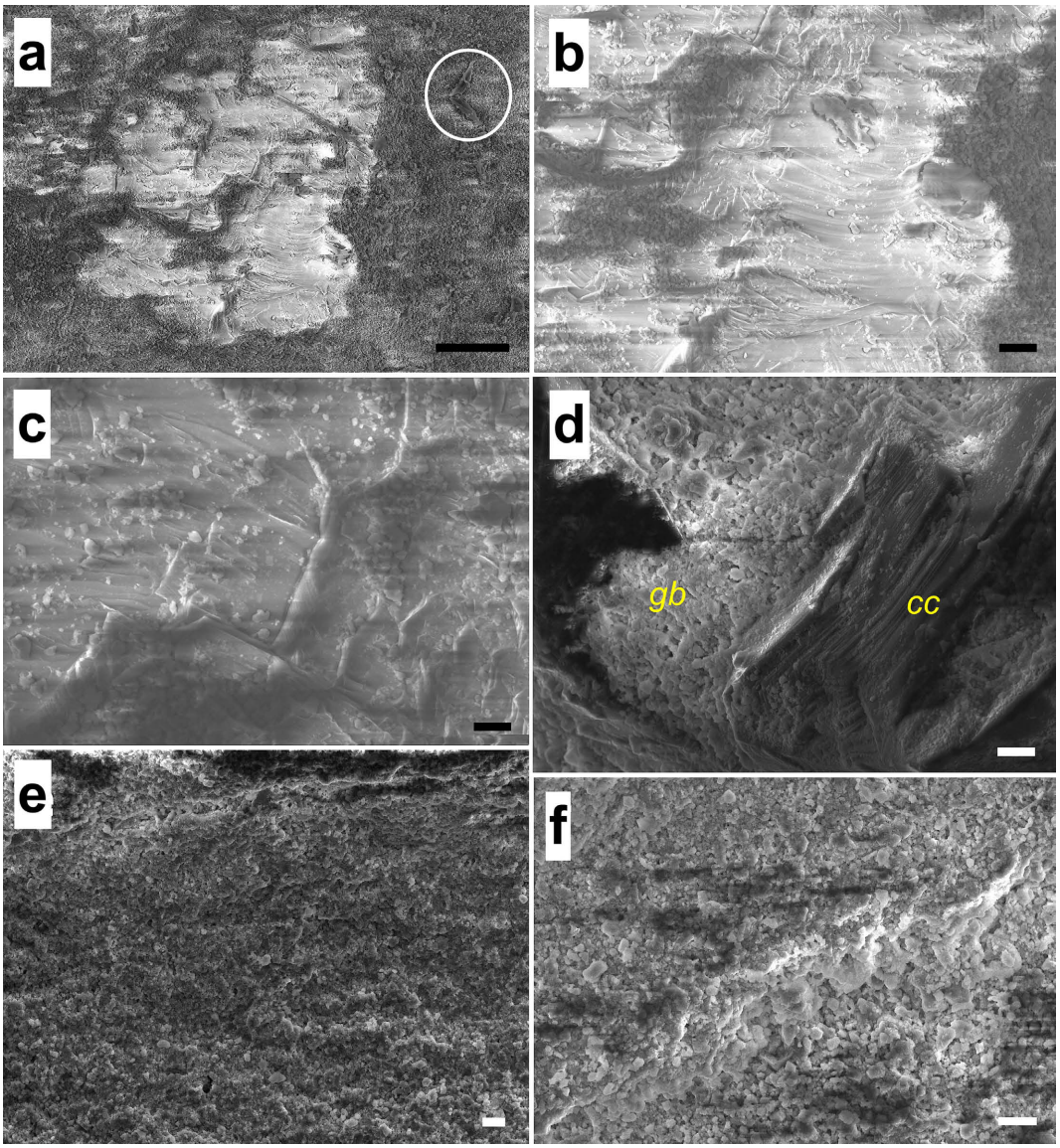

FIGURE 11
Micromorphological preservation of Solnhofen mayflies. SEM images from specimen SMNS 70311a show tissues obliterated by calcite crystals in combination with globular material, or alone. **(A–C)** Calcite crystals between the area in which originally were the head cuticle plates, revealing many cleavage planes, in progressively larger magnifications (120x, 285x, 800x, respectively). Additionally, in 'a' the white circle highlights a possible cuticular element/putative piece of setae. Scale bars 100 µm, 30 µm, and 10 µm, respectively. Voltage 20 kV. WDs 35.98 mm, 36.88 mm, and 36.07 mm, respectively; **(D)** Calcite crystals [cc] between globular material [gb] in the eye; e) Matrix showing globular material; **(F)** Globular material in abdominal segments; **(D–F)** Magnifications 800x, 430x and 850x, respectively. Scale bars 10 µm. Voltage 25kV. WDs 8.8 mm **(D)** and 11.09 mm **(E, F)**.

carcasses' surface (Barling et al., 2020), also mainly composed by goethite, but these fossil insects show worse preservation when compared to pyritized ones (Barling et al., 2020; Bezerra et al., 2020; Dias and Carvalho, 2020; Bezerra and Mendes, 2024).

We report mayfly larvae from the Crato Formation with a wrinkle-like surface in the cuticle of their abdominal terga, which we hypothesize were imprinted after dehydration of the cuticle due to the action of microbial mats. Recently, Dias et al. (2023) showed similar results and hypothesized that the microbial mats created a sealing effect during the coating of the carcasses, causing dehydration, followed by further dehydration during diagenesis. We also show microscopic features that suggest the presence of mats in fossil orthopterans, such as the EPS-like amorphous material covering and filling parts of the preserved inner organs, agreeing with Dias and Carvalho (2022), who reported negative-relief impressions on the cuticle of orthopterans (like the wrinkle-like surfaces shown here), and web-like texture (as the amorphous matter of our specimens) which they also interpreted as EPS originally excreted by microorganisms. These microorganisms produce mucilage, a gelatinous material capable of mobilizing solutions and altering the biogeochemistry of sedimentary environments (Gerdes, 2003). The presence of pseudomorphs of framboidal pyrite replacing insects, in association with putative EPS, corroborates the hypothesis that microbial-mat-forming

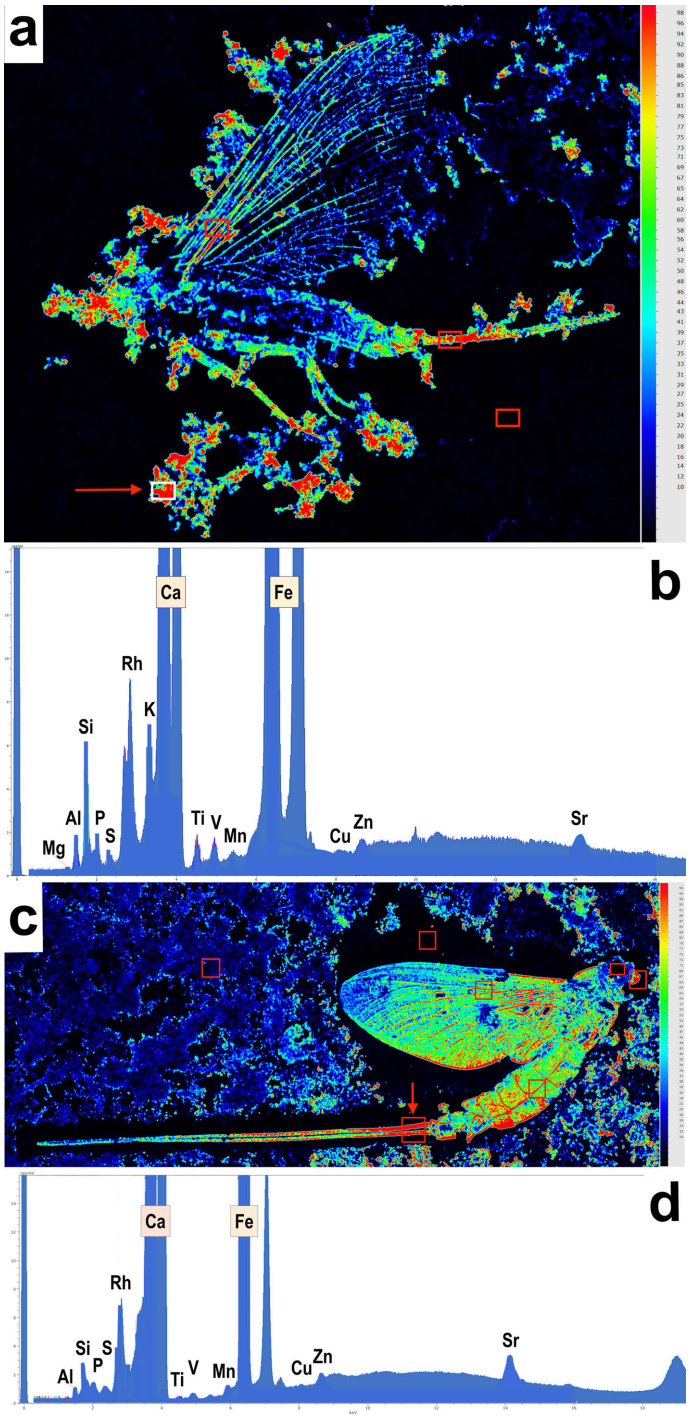

FIGURE 12
µEDXRF intensity maps of Solnhofen mayflies. **(A)** µEDXRF intensity map of iron (Fe) of specimen SMNS 70310, with analyzed spots marked by red rectangles. The intensity is higher towards the reddish colorations. **(B)** Spectrum of the elements recovered at the point highlighted by the arrow in 'a'. **(C)** Intensity map of iron (Fe) of specimen SMNS 70311a, with analyzed spots marked by red rectangles. **(D)** Spectrum measured on the point highlighted by the arrow in 'c'. The intensity maps of the remaining analyzed points are shown in Supplementary Figures F, G.

sulfate-reducing bacteria precipitated the pyrite responsible for the preservation of Crato fossil insects (Briggs, 2003; Wang et al., 2012; Delgado et al., 2014; Barling et al., 2015; Osés et al., 2016; Dias and Carvalho, 2022).

Recently, several works assessed the role of microbial mats on the preservational mechanics of Crato Formation arthropods (Varejão et al., 2019; Iniesto et al., 2021; Dias and Carvalho, 2022). Based on these previous authors and our results, we assume that specialized benthic communities formed microbial mats that proliferated in the lake substrate of the Crato Formation. According to Prieto-Barajas et al. (2018), photosynthesis is the main source of energy and nutrition for a

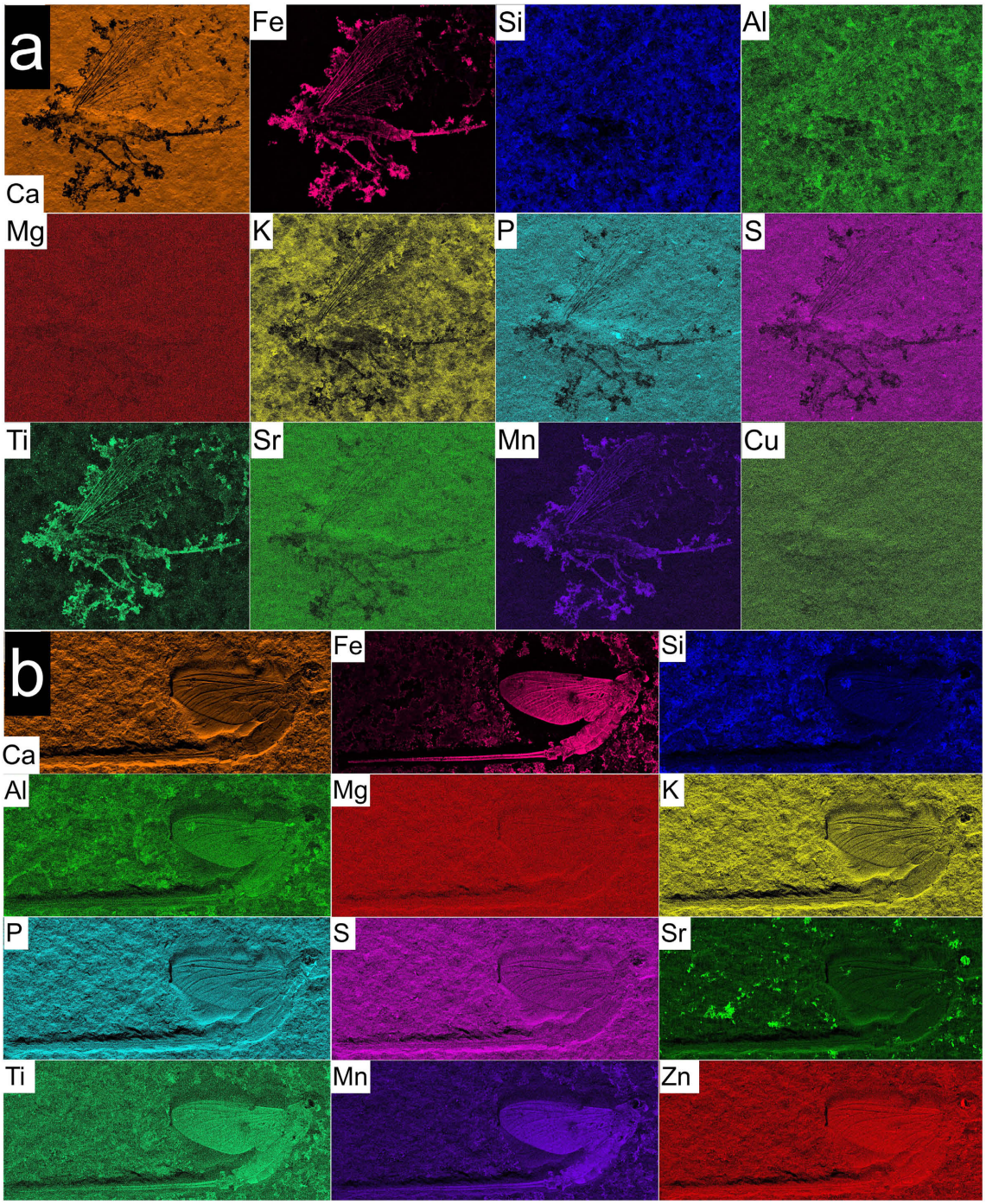

FIGURE 13
μEDXRF distribution maps of elements from Solnhofen mayflies. *Hexagenites* specimens **(A)** SMNS 70310 and **(B)** SMNS 70311a. Ca, calcium; Fe, iron; Si, silicon; Al, aluminum; Mg, magnesium; K, potassium; P, phosphorus; S, sulfur; Sr, strontium; Ti, titanium; Mn, manganese; Zn, zinc; Cu, copper.

microbial mat, which is a limiting factor for its occurrence and distribution across a hypersaline lacustrine environment. Therefore, the waters of the Crato paleolake should have been shallow enough for appropriate luminosity to reach the substrate, allowing photosynthesis of these benthic communities (Varejão et al., 2019).

In addition to pyrite, the occurrence of calcium phosphate, when associated with other microbial features, can also indicate the effect of microbial mats (Noffke and Awramik, 2013; Prieto-Barajas et al., 2018). Wang et al. (2012) reported pyrite halos around insect fossils suggesting the presence of reducing microenvironments facilitated by microbial mats; also, it is known that pyrite is commonly formed during the replication of cells of the microbial mats (Noffke and Awramik, 2013). Dias and Carvalho (2022) inferred that the paleoenvironments of yellowish (with pyritized

insect fossils) and grayish limestones (with kerogenized insect fossils) of the Crato Formation were distinct. The yellowish limestones represent more arid conditions, which are favorable for the development of microbial mats, while the grayish limestones represent more humid conditions, which limits the growth of microbial mats (Dias and Carvalho, 2022).

Since the mayflies of Solnhofen limestones do not present any morphological or preservational signs of previous action of microbial mats during their diagenesis, we assume that microbial mats were not available or, if present, were more restricted in the Solnhofen substrate, similarly to what is hypothesized by Dias and Carvalho (2022) for the grayish layers of the Crato Formation (though those features could also be simply not preserved). However, since almost the entire Solnhofen vertebrate fauna is exceptionally preserved through phosphatization (Wilby and Briggs, 1997; Frey et al., 2003; Klug et al., 2015; Tałanda, 2018; Barlow et al., 2021; Delsett et al., 2022), those mats were likely prospering during probably more arid phases of the basin and thus preserving them.

Unlike the Crato Formation, in which the larval stages of mayflies are dominant (Martins-Neto, 2006; Storari et al., 2021a), no larvae are present in the Solnhofen limestones, which could indicate that their adults were reproducing in stagnant waters in close, emergent lands, and that the carcasses of the adults were washed out directly to the marine depositional site during floodings (Bechly, 2015; Staniczek et al., 2022), or were carried out by the wind. This could also indicate that the marine paleoenvironment was isolated from any adjacent stream (Barthel et al., 1990), suggesting that, at least during the phases when the mayflies were deposited, the Solnhofen water setting was a partly or completely closed system, with restricted water flow (Barthel et al., 1990). This also differs from the Crato Formation, which had streams that flowed into the paleolake where the limestones were deposited (Ribeiro et al., 2021). The great majority of Solnhofen mayflies we studied here are preserved in lateral view, with wings closed at rest, which suggests that dead individuals were transported floating on the water surface (Martínez-Delclòs and Martinell, 1993). An interesting feature of the taphonomic history of Solnhofen mayflies is that, although their preservation is very poor, few specimens are disarticulated, likely due to the low disarticulation rates of specimens in the calm depositional environment (Viohl, 1994). Insects that arrived dead on the depositional site would remain on the surface of the water longer and undergo greater necrolysis until the water tension broke (e.g., through storms), while those that drowned would sink promptly, reaching the bottom faster (Martínez-Delclòs and Martinell, 1993; Martínez-Delclòs et al., 2004). This taphonomic history is, for instance, different from the Solnhofen dragonflies, which are commonly preserved with open wings, a sign that has been interpreted as indicating drowning (Martínez-Delclòs and Martinell, 1993; Barling et al., 2021), and which might account for their good preservation at hand scale compared to the mayflies of this unit (Bechly, 2015).

Although the Solnhofen limestones are exceedingly fine-grained, enabling the preservation of fine details, for example, of the feathers of *Archaeopteryx lithographica* (de Buisonjé, 1985), the preservation of mayflies is very modest, which suggests a different taphonomic history than well-preserved taxonomic groups, or could simply represent different temporal phases of deposition of the basin, with different conditions for fossil diagenesis. Fossil insects from the Solnhofen limestones have been the topic of many studies describing them as being mostly poor-quality (sometimes called 'rough') calcite and pyrolousite casts that retain some three-dimensionality (Ponomarenko, 1985; Viohl, 1990; Martínez-Delclòs et al., 2004; Grimaldi and Engel, 2005), similarly to our results. However, until now, arthropod groups from this unit have lacked any published geochemical characterization. Despite this, Martínez-Delclòs et al. (2004) described Solnhofen as a typical site of phosphatization for insects, as commonly described for vertebrates of this unit (Frey et al., 2003), which we believe is unlikely, at least for the mayflies, since none of the analyzed specimens presented such type of preservation. Instead, we observe that the mineralogy of the Solnhofen mayflies is largely calcitic, with a chemical composition similar to that of the host rock, but with metals associated with the best-preserved parts and no phosphatic influence, differing largely from the pattern observed in the vertebrates (Kundrát et al., 2018; Li et al., 2021). In Solnhofen vertebrates, the rock where the fossil is embedded is usually rich in elements like Si, K, Ca, Ti, Mn, and Fe, with Fe, Mn and Ti being reported as low in the fossils themselves (Kundrát et al., 2018; Li et al., 2021), while Zn had contrasting reports (Bergmann et al., 2010; Li et al., 2021). The preferential association of Fe, Mn, Ti, and Zn with the mayfly fossils we describe here may imply early mineralization of a yet undetermined mineral phase that favored the preservation of some specimens.

Based on our data, we propose hypotheses about the preservation of mayflies in the frame of the Flinz and Fäule phases of the Solnhofen limestones. Fossil mayflies are preserved mainly in the Flinz layers, which are associated with episodes of more humid conditions (Munnecke et al., 2008), suggesting times with more habitats for these aquatic insects near the depositional site. It is also possible that the mayflies are not well-preserved because microbial mats were absent or restricted in the depositional site, compared to Fäule phases, which are associated with drier periods that are ideal for the proliferation of microbial mats (Keupp, 1977; Seilacher et al., 1985; Iniesto et al., 2013, 2015; Viohl, 2015). Hess et al. (1999) noticed that the preservation of *Saccocoma* crinoids is best in the Fäule beds, while in Flinz beds recrystallized calcite obscures their details, similarly to the preservation of mayflies. From the scarcity of fossils in the Flinz beds, Barthel (1978) concluded that these were deposited rapidly, with the bulk of sediments washed in during storms. Based on fish taphonomy, Viohl (1994) similarly inferred very rapid deposition of the Flinz, with several laminae representing less than a year. Flinz periods were followed by quiet, marly Fäule episodes. During such times, cyanobacteria, whose spherical remains occur in some of the Fäule beds, could have formed mats (Hess et al., 1999), which probably explains the exceptional preservation of several fossils in the Fäule beds and the low preservation of mayflies in the Flinz layers.

Similarly to the Flinz and Fäule cycles of the Solnhofen limestones, the Crato Formation also shows different types of limestones related to different sedimentation conditions. The limestones of the Crato Formation bear two laminated facies, the clay-carbonate rhythmite ('dark'), and the laminated limestone ('pale', dominated by calcite crystals), that corresponds to a shift in the depositional balance of authigenic carbonate precipitation and terrigenous input (Neumann et al., 2003; Heimhofer and Martill, 2007). However, within the microfacies the limestones also differ cyclically in mineralogy between yellowish and grayish limestones. Pyritized insects mainly occur in yellowish limestones, while kerogenized fossils are preserved in grayish limestones (Barling et al., 2020), and mayflies are extremely rare in grayish limestones (unpublished results, and Dias et al., 2023). So, contrary to Solnhofen, mayfly fossils are associated with the limestone type that holds the best-preserved insects at the Crato Formation.

5 Conclusion

The application of analytical techniques of spectroscopy was paramount to further unravel the fossil preservation in the studied Lagerstätten. An intimate relationship is observed between insect soft tissue preservation and fine-grained laminated carbonates, such as those of the Crato Formation and Solnhofen limestones (Martínez-Delclòs et al., 2004).

The preservation of Crato mayflies and crickets is more diverse, with fossils displaying calcium phosphate and iron oxides/hydroxides preserving internal features, and the majority of specimens being, in general, substituted by iron oxide after pyritization, though in rare cases they can be preserved by carbonaceous content in grayish limestone (Dias and Carvalho, 2020). Additionally, we could differentiate the mineralogy between the cuticle and the well-preserved internal organs of some specimens. The high-fidelity preservation of internal organs is due to smaller, closely-packed framboids compared to the cuticle and other less-preserved parts. In our results, Crato specimens presented microscopic features that suggest the presence of microbial mats during the fossilization process, such as micro cracks, wrinkles, and EPS-like amorphous matter covering and infilling voids.

In comparison to the Crato insects, the mayfly fossils of the Solnhofen limestones show, at their highest fidelity, that they are complete, fully-articulated, but with no submicron-scale replication of either external or internal morphology. The preservational fabric is largely calcitic imprints with metal influence, which are, for the first time, described as a preservation mode for Solnhofen fossil insects. We recovered no phosphatic influence, as common for their vertebrates, for instance. Based on their biostratinomy, we hypothesize that the mayflies were deposited in a partly or completely closed system with restricted water flow and that the specimens arrived dead on the water surface or were brought by winds. Also, their low preservation probably occurred during episodic humid conditions, and with restricted or no action of microbial mats.

Data availability statement

The original contributions presented in the study are included in the article/Supplementary Material. Further inquiries can be directed to the corresponding author.

Author contributions

AS: Conceptualization, Data curation, Formal analysis, Investigation, Project administration, Validation, Visualization, Writing – original draft, Writing – review & editing. GO: Data curation, Formal analysis, Investigation, Software, Validation, Visualization, Writing – review & editing. AS: Data curation, Resources, Supervision, Writing – review & editing. MR: Formal analysis, Resources, Writing – review & editing. RL: Formal analysis, Writing – review & editing. TR: Conceptualization, Data curation, Funding acquisition, Project administration, Resources, Supervision, Visualization, Writing – review & editing.

Funding

The author(s) declare financial support was received for the research, authorship, and/or publication of this article. The present paper contains the results of a research project that received funding for the stay of APS at the SMNS by the German Academic Exchange Service (DAAD), under grant No. 91808123. This study was financed in part by the Coordenação de Aperfeiçoamento de Pessoal de Nível Superior (CAPES – Finance Code 001) to APS. TR thanks Fundação de Amparo à Pesquisa e Inovação do Espírito Santo and Conselho Nacional de Desenvolvimento Científico e Tecnológico (FAPES/CNPq, grant 509/2020), and Conselho Nacional de Desenvolvimento Científico e Tecnológico (CNPq, grant 314260/2021–8). GLO thanks the "Programa de Pós-Doutorado" and the "Programa Pesquisador Colaborador" from the IF-USP. GLO acknowledges the São Paulo Research Foundation (FAPESP) for the grants #2021/07007-7, #2023/14250-0 and #2022/06485-5.

Acknowledgments

We thank Antônio Álamo Saraiva, Renan Bantim, and Allysson Pinheiro for access to collections of the MPPCN in Santana do Cariri and LPU in Crato, as well as Lucio Silva for receiving APS in the MPPCN accommodations. We also thank Juliana Sayão for access to the specimen from the CAV. We acknowledge Johannes Giebel for μEDXRF analyses at the Technische Universität Berlin, and Cristina Gascó Martín for technical support during some SEM test analyses at the SMNS. We thank the Centro de Pesquisas em Geocronologia e Geoquímica Isotópica, IGc-USP, and particularly Isaac Jamil Sayeg for support during SEM analyses, as well as Evandro Pereira and Fabio Rodrigues for support in the use of the Raman equipment at the IQ-USP. We thank Christina Ifrim (JME), Markus Moser (SNSB-BSPG), Martin Röper (BMMS), Georg Bérger (MB), and Eberhard

Frey (SMNK) for kindly granting access to the scientific collections of Solnhofen mayflies. Special thanks also to Mónica Solórzano-Kraemer (SMF) for support and loan of Solnhofen material. We acknowledge Juliana Leme and Ivone Cardoso Gonzales for the permission to study specimens from the Paleontological Scientific Collection, University of São Paulo, and for research support. We thank Mírian Pacheco for her valuable comments on an earlier version of the manuscript. We also thank the topic editors of Frontiers in Ecology and Evolution for organizing this special edition.

Conflict of interest

The authors declare that the research was conducted in the absence of any commercial or financial relationships that could be construed as a potential conflict of interest.

Publisher's note

Supplementary material

The Supplementary Material for this article can be found online at: https://www.frontiersin.org/articles/10.3389/fevo.2024.1445160/full#supplementary-material

References

Arai, M., and Assine, M. L. (2020). Chronostratigraphic constraints and paleoenvironmental interpretation of the Romualdo Formation (Santana Group, Araripe Basin, Northeastern Brazil) based on palynology. *Cretaceous Res.* 116, 104610. doi: 10.1016/j.cretres.2020.104610

Assine, M. L. (2007). Bacia do araripe. *Boletim Geociências Petrobras* 15, 371–389.

Assine, M., Perinotto, A., Custódio, M. A., Neumann, V., Varejão, F. G., and Mescolotti, P. C. (2014). Sequências Deposicionais do Andar Alagoas (Aptiano superior) da Bacia do Araripe, Nordeste do Brasil. *Boletim Geociências Petrobras* 22, 3–28.

ASTM International (2002). Standard guide for Raman shift standards for spectrometer calibration. *Annu. B. ASTM Stand.* 96, 1–11.

Barling, N. T., Heads, S. W., and Martill, D. M. (2021). Behavioural impacts on the taphonomy of dragonflies and damselflies (Odonata) from the Lower Cretaceous Crato Formation, Brazil. *Palaeoentomology* 4, 141–155. doi: 10.11646/palaeoentomology.4.2.3

Barling, N., Martill, D. M., and Heads, S. W. (2020). A geochemical model for the preservation of insects in the Crato Formation (Lower Cretaceous) of Brazil. *Cretaceous Res.* 116, 104608. doi: 10.1016/j.cretres.2020.104608

Barling, N., Martill, D. M., Heads, S. W., and Gallien, F. (2015). High fidelity preservation of fossil insects from the Crato Formation (Lower Cretaceous) of Brazil. *Cretaceous Res.* 52, 605–622. doi: 10.1016/j.cretres.2014.05.007

Barlow, L. A., Pittman, M., Butcher, A., Martill, D., and Kaye, T. G. (2021). Laser-stimulated fluorescence reveals unseen details in fossils from the Upper Jurassic Solnhofen Limestones. *R. Soc. Open Sci.* 8 (12), 211601. doi: 10.1098/rsos.211601

Barthel, K. W. (1978). *Solnhofen – Ein Blick in die Erd-geschichte* (Thun: Ott Verlag), 393 pp.

Barthel, K. W., Swinburne, N. H. M., and Conway-Morris, S. (1990). *Solnhofen: a study in Mesozoic palaeontology* (Cambridge: Cambridge University Press), 236 pp.

Bausch, W. M. (2004). Geochemie des profils Maxberg/Solnhofen. *Erlanger Beitr. Petr. Min.* 14, 35–51.

Bausch, W. M., Viohl, G., Bernier, P., Barale, G., Bourseau, J. P., Buffetaut, E., et al. (1994). Eichstätt and Cerin: geochemical comparison and definition of two different Plattenkalk types. *Geobios* 16, 107–125. doi: 10.1016/S0016-6995(94)80026-X

Bechly, G. (2015). "Insekten (Hexapoda)," in *Solnhofen. Ein Fenster in die Jurazeit*. Eds. G. Arratia, H. P. Schultze, H. Tischlinger and G. Viohl (Verlag Dr. Friedrich Pfeil, Munich), 239–270.

Bergmann, U., Morton, R. W., Manning, P. L., Sellers, W. I., Farrar, S., Huntley, K. G., et al. (2010). Archaeopteryx feathers and bone chemistry fully revealed via synchrotron imaging. *Proc. Natl. Acad. Sci. U.S.A* 107, 9060–9065. doi: 10.1073/pnas.1001569107

Beurlen, K. A. (1962). Geologia da Chapada do Araripe. *Anais da Academia Bras. Cienc.* 34, 365–370.

Bezerra, F. I., Da Silva, J. H., Agressot, E. V. H., Freire, P. T. C., Viana, B. C., and Mendes, M. (2023). Effects of chemical weathering on the exceptional preservation of mineralized insects from the Crato Formation, Cretaceous of Brazil: implications for late diagenesis of fine-grained Lagerstätten deposits. *Geological Magazine* 160, 911–926. doi: 10.1017/s0016756823000043

Bezerra, F. I., Da Silva, J. H., De Paula, A. J., Oliveira, N. C., Paschoal, A. R., Freire, P. T. C., et al. (2018). Throwing light on an uncommon preservation of Blattodea from the Crato Formation (Araripe Basin, Cretaceous), Brazil. *Rev. Bras. Paleontologia* 21, 245–254. doi: 10.4072/rbp.2018.3.05

Bezerra, F. I., Da Silva, J. H., Miguel, E. C., Paschoal, A. R., Nascimento, D. R. Jr., Freire, P. T. C., et al. (2020). Chemical and mineral comparison of fossil insect cuticles from Crato Konservat Lagerstätte, Lower Cretaceous of Brazil. *J. Iberian Geol.* 46, 61–76. doi: 10.1007/s41513-020-00119-y

Bezerra, F. I., and Mendes, M. (2024). A palaeoecological analysis of the Cretaceous (Aptian) insect fauna of the Crato Formation, Brazil. *Palaeogeogr. Palaeoclimatol. Palaeoecol.* 641, 112134. doi: 10.1016/j.palaeo.2024.112134

Bezerra, F. I., Solórzano-Kraemer, M. M., and Mendes, M. (2021). Distinct preservational pathways of insects from the Crato Formation, Lower Cretaceous of the Araripe Basin, Brazil. *Cretaceous Res.* 118, 104631. doi: 10.1016/j.cretres.2020.104631

Bragg, W. L. (1924). "The structure of aragonite," in *Proceedings of the Royal Society of London. Series a, Containing Papers of a Mathematical and Physical Character*, vol. 105, 16–39. doi: 10.1098/rspa.1924.0002

Brandão, N. C., Bittencourt, J. S., Calor, A. R., Mendes, M., and Langer, M. C. (2021). The Ephemeroptera (Hexapoda, Insecta) from the Lower Cretaceous Crato Formation (NE Brazil): a new genus and species, and reassessment of *Costalimella zucchii* Zamboni 2001 and Cratogenites corradiniae Martins-Neto 1996. *Cretaceous Res.* 127, 104923. doi: 10.1016/j.cretres.2021.104923

Briggs, D. E. G. (2003). "The role of biofilms in the fossilization of non-biomineralized tissues," in *Fossil and recent biofilms: a natural history of life on Earth*. Eds. W. E. Krumbein, D. M. Paterson and G. A. Zarvarzin (Kluwer Acad. Publ, Dordrecht), 281–290.

Briggs, D. E. G., Kear, A. J., Martill, D. M., and Wilby, P. (1993). Phosphatization of softtissue in experiments and fossils. *J. Geological Soc.* 150, 1035e1038.

Brito, I. M. (1987). "Nota preliminar sobre uma nova Efemera do Cretaceo do Ceara (Insecta Ephemeroptera)," in *Anais do X Congresso Brasileiro de Paleontologia*, Rio de Janeiro, 593–597.

Catto, B., Jahnert, R. J., Warren, L. V., Varejão, F. G., and Assine, M. L. (2016). The microbial nature of laminated limestones: Lessons from the Upper Aptian, Araripe Basin, Brazil. *Sedimentary Geol.* 341, 304–315. doi: 10.1016/j.sedgeo.2016.05.007

Chen, L., Xiao, S., Pang, K., Zhou, C., and Yuan, X. (2014). Cell differentiation and germ–soma separation in Ediacaran animal embryo-like fossils. *Nature* 516, 238–241. doi: 10.1038/nature13766

Coimbra, J. C., and Freire, T. M. (2021). Age of the Post-rift Sequence I from the Araripe Basin, Lower Cretaceous, NE Brazil: implications for spatio-temporal correlation. *Rev. Bras. Paleontologia* 24, 37–46. doi: 10.4072/rbp.2021.1.03

de Buisonjé, P. H. (1985). "Climatological conditions during deposition of the Solnhofen limestones. 45-65," in *The beginnings of birds. Proceedings of the International* Archaeopteryx *Conference, Eichstät*. Eds. M. K. Hecht, J. H. Ostrom, G. Viohl and P. Wellnhofer (Freunde des Jura-Museums Eichstätt, Eichstätt), 382 pp.

Delgado, A. O., Buck, P. V., Osés, G., Ghilardi, R. P., Rangel, E. C., and Pacheco, M. L. (2014). Paleometry: A brand new area in Brazilian science. *Mater. Res.* 17, 1434–1441. doi: 10.1590/1516-1439.288514

Delsett, L. L., Friis, H., Kölbl-Ebert, M., and Hurum, J. H. (2022). The soft tissue and skeletal anatomy of two Late Jurassic ichthyosaur specimens from the Solnhofen archipelago. *PeerJ* 10, e13173. doi: 10.7717/peerj.13173

Dias, J. J., and Carvalho, I. S. (2020). Remarkable fossil crickets preservation from Crato Formation (Aptian, Araripe Basin), a Lagerstätten from Brazil. *J. South Am. Earth Sci.* 98, 102443. doi: 10.1016/j.jsames.2019.102443

Dias, J. J., and Carvalho, I. S. (2022). The role of microbial mats in the exquisite preservation of Aptian insect fossils from the Crato Lagerstätte, Brazil. *Cretaceous Res.* 130, 105068. doi: 10.1016/j.cretres.2021.105068

Dias, J. J., Carvalho, I. S., Buscalioni, A. D., Umamaheswaran, R., López-Archilla, A. N., Prado, G., et al. (2023). Mayfly larvae preservation from the Early Cretaceous of Brazilian Gondwana: Analogies with modern mats and other Lagerstätten. *Gondwana Res.* 124, 188–205. doi: 10.1016/j.gr.2023.07.007

Duncan, I. J., and Briggs, D. E. G. (1996). Three-dimensionally preserved insects. *Nature* 381, 30–31. doi: 10.1038/381030b0

Duncan, I. J., Briggs, D. E. G., and Archer, M. (1998). Three-dimensionally mineralised insects and millipedes from the Tertiary of Riversleigh, Queensland, Australia. *Palaeontology* 41, 835–851.

Eriksson, M., Terfelt, F., Elofsson, R., and Marone, F. (2012). Internal soft-tissue anatomy of Cambrian 'Orsten' Arthropods as revealed by synchrotron X-ray tomographic microscopy. *PloS One* 7, e42582. doi: 10.1371/journal.pone.0042582

Fielding, S., Martill, D. M., and Naish, D. (2005). Solnhofen-style soft-tissue preservation in a new species of turtle from the Crato Formation (Early Cretaceous, Aptian) of north-east Brazil. *Palaeontology* 48, 1301–1310. doi: 10.1111/j.1475-4983.2005.00508.x

Frey, D., Tishlinger, H., Buchy, M., and Martill, D. M. (2003). "New specimens of Pterosauria (Reptilia) with soft parts with implications for pterosaurian anatomy and locomotion. 233-266," in *Evolution and palaeobiology of pterosaurs*. Geological Society. Eds. E. Buffetaut and J. M. Mazin (Special Publication, London), 217, 347 pp.

Frickhinger, K. A. (1994). *Die Fossilien von Solnhofen: Dokumentation der aus den Plattenkalken bekannten Tiere und Pflanzen (The fossils of Solnhofen)* (Korb.: Goldschneck), 336.

Frickhinger, K. A. (1999). *Die Fossilien von Solnhofen, 2* (Korb: Goldschneck), 190.

Gerdes, G. (2003). "Biofilms and macroorganisms," in *Fossil and Recent Biofilms: A Natural History of Life on Earth*. Eds. W. E. Krumbein, D. M. Paterson and G. A. Zavarzin (Springer-Science & Business Media, Dordrecht), 197–216.

Gobbo, S. R., and Bertini, R. J. (2013). Tecidos moles (não resistentes): como se fossilizam? *Terrae didatica* 10, 2–13.

Gomes, A. L. S., Becker-Kerber, B., Osés, G. L., Prado, G., Becker-Kerber, P., Barros, G. E. B., et al. (2019). Paleometry as a key tool to deal with paleobiological and astrobiological issues: some contributions and reflections on the Brazilian fossil record. *Int. J. Astrobiol.* 18 (6), 1–15. doi: 10.1017/S1473550418000538

Grimaldi, D. A. (1990). Insects from the santana formation, lower cretaceous, of Brazil. *B Am. Mus. Nat. Hist.* 195, 1–191.

Grimaldi, D. A., and Engel, M. S. (2005). *Evolution of the Insects* (New York: Cambridge University Press), 755 p.

Grimes, S. T., Davies, K. L., Butler, I. B., Brock, F., Edwards, D., Rickard, D., et al. (2002). Fossil plants from the Eocene London Clay: the use of pyrite textures to determine the mechanism of pyritization. *J. Geological Soc.* 159, 493–501. doi: 10.1144/0016-764901-176

Heimhofer, U., Ariztegui, D., Lenniger, M., Hesselbo, S. P., Martill, D. M., Rios-Netto, A. M., et al. (2010). Deciphering the depositional environment of the laminated Crato fossil beds (Early Cretaceous, Araripe Basin, North-eastern Brazil). *Sedimentology* 57, 677–694. doi: 10.1111/j.1365-3091.2009.01114.x

Heimhofer, U., and Martill, D. M. (2007). "The sedimentology and depositional environment of the Crato Formation," in *The Crato Fossil Beds of BRAZIL*. Eds. D. M. Martill, G. Bechly and R. F. Loveridge (Cambridge University Press, Cambridge), 44–62.

H. Hess, W. I. Ausich, C. E. Brett and M. J. Simms (Eds.) (1999). *Fossil Crinoids* (Cambridge, New York, Melbourne: Cambridge University Press).

Heyng, A., Rothgaenger, M., and Röper, M. (2015). "Die grabung brunn," in *Solnhofen. Ein Fenster in die Jurazeit*. Eds. G. Arratia, H.-P. Schultze, H. Tischlinger and G. Viohl (Verlag Dr. Friedrich Pfeil, Munich), 114–118.

Iniesto, M., Gutierrez-Silva, P., Dias, J. J., Carvalho, I. S., Buscalioni, A. D., and López-Archilla, A. I. (2021). Soft tissue histology of insect larvae decayed in laboratory experiments using microbial mats: Taphonomic comparison with Cretaceous fossil insects from the exceptionally preserved biota of Araripe, Brazil. *Palaeogeogr. Palaeoclimatol. Palaeoecol.* 564, 110156. doi: 10.1016/j.palaeo.2020.110156

Iniesto, M., Laguna, C., Florín, M., Guerrero, M. C., Chicote, A., Buscalioni, A. D., et al. (2015). The impact of microbial mats and their microenvironmental conditions in early decay of fish. *Palaios* 30, 792–801. doi: 10.2110/palo.2014.086

Iniesto, M., Lopez-Archilla, A. I., Fregenal-Martinez, M., Buscalioni, A. D., and Carmen-Guerrero, M. (2013). Involvement of microbial mats in delayed decay: An experimental essay on fish preservation. *Palaios* 28, 56–66. doi: 10.2110/palo.2011.p11-099r

Keupp, H. (1977). Ultrafazies und Genese der Solnhofener Plattenkalke. *Abh. Naturhist. Ges. Nürnberg e.V.* 37, 1–127.

Klug, C., Fuchs, D., Schweigert, G., Röper, M., and Tischlinger, H. (2015). New anatomical information on arms and fins from exceptionally preserved Plesioteuthis (Coleoidea) from the Late Jurassic of Germany. *Swiss J. Palaeontol.* 134, 245–255. doi: 10.1007/s13358-015-0093-y

Kundrát, M., Nudds, J., Kear, B. P., Lü, J., and Ahlberg, P. (2018). The first specimen ofArchaeopteryxfrom the Upper Jurassic Mörnsheim Formation of Germany. *Historical Biol.* 31, 3–63. doi: 10.1080/08912963.2018.1518443

Lafuente, B., Downs, R. T., Yang, H., and Stone, N. (2015). "The power of databases: the RRUFF project," in *Highlights in Mineralogical Crystallography*. Eds. T. Armbruster and R. M. Danisi (W. De Gruyter, Berlin, Germany), 1–30.

Leakey, L. S. B. (1952). Lower miocene invertebrates from Kenya. *Nature* 169, 624–625. doi: 10.1038/169624b0

Li, S., and Hihara, L. H. (2015). A Micro-Raman Spectroscopic study of marine atmospheric corrosion of Carbon Steel: The effect of Akaganeite. *J. Electrochemical Soc.* 162, C495–C502. doi: 10.1149/2.0881509jes

Li, J., Pei, R., and Xu, X. (2021). Micro-XRF study of the troodontid dinosaur Jianianhualong Tengi reveals new biological and taphonomical signals. *Atomic Spectrosc.* 41, 1–11. doi: 10.46770/as.2021.01.001

Lima, F. J., Pires, E. F., Saraiva, A. Á. F., Sayão, J. M., Jasper, A., and Uhl, D. (2021). *Early Cretaceous (Aptian–Albian) wildfires in the Araripe basin, northeast Brazil: palaeoclimatic and palaeoenvironmental implications* (Cham: Springer eBooks), 1–12. doi: 10.1007/978-3-319-90913-4_32-1

Maas, A., Braun, A., Dong, X.-P., Donoghue, P. C. J., Müller, K. J., Olempska, E., et al. (2006). The 'Orsten'–More than a Cambrian Konservat-Lagerstätte yielding exceptional preservation. *Palaeoworld* 15, 266–282. doi: 10.1016/j.palwor.2006.10.005

Martill, D. M., Loveridge, R., and Heimhofer, U. (2007). Halite pseudomorphs in the Crato Formation (Early Cretaceous, Late Aptian–Early Albian), Araripe Basin, northeast Brazil: further evidence for hypersalinity. *Cretaceous Res.* 28, 613–620. doi: 10.1016/j.cretres.2006.10.003

Martill, D. M., Loveridge, R. F., and Heimhofer, U. (2008). Dolomite pipes in the Crato Formation fossil lagerstätte (Lower Cretaceous, Aptian), of northeastern Brazil. *Cretaceous Res.* 29, 78–86. doi: 10.1016/j.cretres.2007.04.007

Martill, D. M., and Wilby, P. R. (1993). "Stratigraphy," in *Fossils of the Santana and Crato Formations, BRAZIL. Field Guides to Fossils No. X*. Ed. D. M. Martill (Palaeontological Association, London), 159.

Martínez-Delclòs, X., and Martinell, J. (1993). Insect taphonomy experiments: their application to the Cretaceous outcrops of lithographic limestones from Spain. *Kaupia* 2, 133–144.

Martins-Neto, R. G. (1996). New mayflies (Insecta, Ephemeroptera) from the Santana Formation (Lower Cretaceous), Araripe Basin, northeastern Brazil. *Rev. Española Paleontologia* 11, 177–192.

Martins-Neto, R. G. (2005). Estágio atual da paleoartropodologia Brasileira: hexápodes, miriápodes, crustáceos (Isopoda, Decapoda, Eucrustacea e Copepoda) e quelicerados. *Arquivos do Museu Nacional* 63, 471–494.

Martins-Neto, R. G. (2006). Insetos fósseis como bioindicadores em depósitos sedimentares: um estudo de caso para o Cretáceo da Baciado Araripe (Brasil). *Rev. Bras. Zoociências* 8, 155–183.

Martínez-Delclòs, X., Briggs, D. E. G., and Peñalver, E. (2004). Taphonomy of insects in carbonates and amber. *Palaeogeogr. Palaeoclimatol. Palaeoecol.* 203, 19–64. doi: 10.1016/s0031-0182(03)00643-6

McCafferty, W. P. (1990). "Chapter 2. Ephemeroptera," in *Bulletin of the American Museum of Natural History*, New York, vol. 195, 20–50.

McCobb, L. M. E., Duncan, I. J., Jarzembowski, E. A., Stankiewicz, B. A., Wills, M. A., and Briggs, D. E. G. (1998). Taphonomy of the insects from the Insect Bed (Bembridge Marls), late Eocene, Isle of Wight, England. *Geological Magazine* 135, 553–563. doi: 10.1017/s0016756898001204

Melo, R. M., Guzman, J., Almeida-Lima, D., Piovesan, E. K., Neumann, V. H. M. L., and Sousa, A. J. (2020). New marine data and age accuracy of the Romualdo Formation, Araripe Basin, Brazil. *Sci. Rep.* 10, 1–15. doi: 10.1038/s41598-020-72789-8

Menges, F. (2022). *Spectragryph - optical spectroscopy software, Version 1.2.16.1*.

Menon, F., and Martill, D. M. (2007). "Taphonomy and preservation of Crato Formation arthropods," in *The Crato Fossil Beds of Brazil: Window into an ancient world*. Eds. D. M. Martill, G. Bechly and R. F. Loveridge (Cambridge: Cambridge University Press), 79–96.

Moura-Júnior, D. A., Scheffler, S. M., Moreira, F. F., Nel, A., and Mejdalani, G. (2020). First record of a shore bug (Insecta, Hemiptera, Saldidae) from Gondwana. *J. Paleontol.* 95, 133–140. doi: 10.1017/jpa.2020.61

Munnecke, A., Westphal, H., and Kölbl-ebert, M. (2008). Diagenesis of plattenkalk: examples from the Solnhofen area (Upper Jurassic, southern Germany). *Sedimentology* 55, 1931–1946. doi: 10.1111/j.1365-3091.2008.00975.x

Nel, A., and Pouillon, J.-M. (2020). The third skimmer dragonfly species from the Lower Cretaceous (Aptian) Crato Formation in NE Brazil (Odonata, Cavilabiata, Araripelibellulidae). *Cretaceous Res.* 115, 104565. doi: 10.1016/j.cretres.2020.104565

Neumann, V. H., Borrego, A. G., Cabrera, L., and Dino, R. (2003). Organic matter composition and distribution through the Aptian–Albian lacustrine sequences of the Araripe Basin, northeastern Brazil. *Int. J. Coal Geol.* 54, 21–40. doi: 10.1016/S0166-5162(03)00018-1

Neumann, V. H., and Cabrera, L. (1999). Una nueva propuesta estratigráfica para la tectonosecuencia post-rifte de la cuenca de Araripe, nordeste de Brasil. *Boletim do 5° Simpósio sobre o Cretáceo do Brasil*, 279–285.

Niebuhr, B., and Pürner, T. (2014). Lithostratigraphie der Weißjura-Gruppe der Frankenalb (außeralpiner Oberjura) und der mittel- bis oberjurassischen Reliktvorkommen zwischen Straubing und Passau (Bayern). *Schriftenreihe der Deutschen Gesellschaft für Geowissenschaften* 83, 5–72. doi: 10.1127/sdgg/83/2014/5

Noffke, N., and Awramik, S. M. (2013). Stromatolites and MISS—Differences between relatives. *GSA Today* 23, 4–9. doi: 10.1130/gsatg187a.1

Oliveira, G. R., and Kellner, A. W. A. (2017). Rare hatchling specimens of Araripemys Price 1973 (Testudines, Pelomedusoides, Araripemydidae) from the Crato Formation, Araripe Basin. *J. South Am. Earth Sci.* 79, 137–142. doi: 10.1016/j.jsames.2017.07.014

Osés, G. L., Petri, S., Becker-Kerber, B., Romero, G. R., Rizzutto, M. A., Rodrigues, F., et al. (2016). Deciphering the preservation of fossil insects: a case study from the Crato Member, Early Cretaceous of Brazil. *PeerJ* 4, e2756. doi: 10.7717/peerj.2756

Osés, G. L., Petri, S., Voltani, C. G., Prado, G. M. E. M., Galante, D., Rizzutto, M. A., et al. (2017). Deciphering pyritization-kerogenization gradient for fish soft-tissue preservation. *Sci. Rep.* 7, 1468. doi: 10.1038/s41598-017-01563-0

Palmer, A. R. (1957). "Miocene arthropods from the Mojave desert California," in *Geological survey professional paper 294-G* (United States Government Printing Office, Washington).

Pan, Y., Hu, L., and Zhao, T. (2018). Applications of chemical imaging techniques in paleontology. *Natl. Sci. Review/National Sci. Rev.* 6, 1040–1053. doi: 10.1093/nsr/nwy107

Park, M. H., and Fürsich, F. T. (2002). Stable isotopes and trace element compositions of the Upper Jurassic Solnhofen platy limestone. *Geosci. J.* 6, 269–276.

Parker, A. R., and McKenzie, D. R. (2003). The cause of 50 million-year-old colour. *Proc. - R. Society Biol. Sci.* 270, 151–153. doi: 10.1098/rsbl.2003.0055

Perardi, A., Zoppi, A., and Castellucci, E. (2000). Micro-Raman spectroscopy for standard and in *situ* characterisation of painting materials. *J. Cultural Heritage* 1, 269–272. doi: 10.1016/S1296-2074(00)00176-X

Ponomarenko, A. G. (1985). *Fossil insects from the Tithonian "Solnhofener Plattenkalke" in the Museum of Natural History* Vol. 87 (Vienna: Annalen Naturhistorische Museum Wien), 135–144.

Pouillon, J.-M., and Nel, A. (2020). The oldest representative of the modern clade Aeshnodea from the Lower Cretaceous Crato Formation, Araripe Basin, NE Brazil (Odonata: Anisoptera). *Cretaceous Res.* 116, 104580. doi: 10.1016/j.cretres.2020.104580

Prado, G., Arthuzzi, J. C. L., Osés, G. L., Callefo, F., Maldanis, L., Sucerquia, P., et al. (2021). Synchrotron radiation in palaeontological investigations: Examples from Brazilian fossils and its potential to South American palaeontology. *J. South Am. Earth Sci.* 108, 102973. doi: 10.1016/j.jsames.2020.102973

Prieto-Barajas, C. M., Valencia-Cantero, E., and Santoyo, G. (2018). Microbial mat ecosystems: Structure types, functional diversity, and biotechnological application. *Electronic J. Biotechnol.* 31, 48–56. doi: 10.1016/j.ejbt.2017.11.001

Ribeiro, A. C., Ribeiro, G. C., Varejão, F. G., Battirola, L. D., Pessoa, E. M., Simões, M. G., et al. (2021). Towards an actualistic view of the Crato Konservat-Lagerstätte paleoenvironment: A new hypothesis as an Early Cretaceous (Aptian) equatorial and semi-arid wetland. *Earth-sci. Rev.* 216, 103573. doi: 10.1016/j.earscirev.2021.103573

Röper, M. (2005). Field Trip B: East Bavarian plattenkalk – different types of Upper Kimmeridgian to Lower Tithonian plattenkalk deposits and facies. *Zitteliana B* 26, 57–70.

Röper, M., and Rothgaenger, M. (1995). "Eine neue Fossillagerstätte in den ostbayerischen Oberjura-Plattenkalken bei Brunn/Oberpfalz. Erster Forschungsbericht," in *Freunde der Bayerischen Staatssammlung für Paläontologie und Historische Geologie eV, Jahresbericht und Mitteilungen*, München, vol. 24. , 32–46.

Santos, M. F. A., Mattos, I., Mermudes, J. R. M., Scheffler, S. M., and Reyes-Castillo, P. (2021). A new passalid fossil (Insecta: Coleoptera) from the Santana Formation (Crato member, Lower Cretaceous), Araripe Basin, NE Brazil: Paleoecological and paleobiogeographic implications. *Cretaceous Res.* 118, 104664. doi: 10.1016/j.cretres.2020.104664

Saraiva, A. A. F., Lima, F. J., Barros, O. A., and Bantim, R. A. M. (2021). *Guia de fósseis da Bacia do Araripe* (Crato: Ceará), 378 pp.

Schlüter, T., Kohring, R., and Gregor, H.-J. (2002). Dragonflies preserved in transparent gypsum crystals from the Messinian (Upper Miocene) of Alba, northern Italy. *Acta Zoologica Cracoviensia* 46, 373–379.

Schweigert, G. (2007). Ammonite biostratigraphy as a tool for dating Upper Jurassic lithographic limestones from South Germany – first results and open questions. *Neues Jahrbuch für Geologie und Paläontologie* 245, 117–125. doi: 10.1127/0077-7749/2007/0245-0117

Schweigert, G. (2015). "Biostratigraphie der Plattenkalke der südlichen Frankenalb," in *Solnhofen. Ein Fenster in die Jurazeit*. Eds. G. Arratia, H. P. Schultze, H. Tischlinger and G. Viohl (Verlag Dr. Friedrich Pfeil, Munich), 63–66.

Schwermann, A. H., Rolo, T. S., Caterino, M. S., Bechly, G., Schmied, H., Baumbach, T., et al. (2016). Preservation of three-dimensional anatomy in phosphatized fossil arthropods enriches evolutionary inference. *eLife* 5, e12129. doi: 10.7554/elife.12129

Seilacher, A., Reif, W. E., and Westphal, F. (1985). Sedimentological, ecological and temporal patterns of Fossil-Lagerstätten. *Philos. Trans. R. Soc. London* 311, 5–23.

Staniczek, A. H. (2007). "Ephemeroptera: mayflies," in *The Crato Fossil Beds of Brazil*. Eds. D. M. Martil, G. Bechly and R. F. Loveridge (Cambridge University Press, Cambridge), 163–184.

Staniczek, A. H., Storari, A. P., and Godunko, R. J. (2022). Revised systematics, phylogeny, and paleontology of the mayfly family Baetiscidae (Insecta: Ephemeroptera). *Arthropod Sys. Phylogeny* 80, 389–409. doi: 10.3897/asp.80.e82845

Storari, A. P., Godunko, R. J., Salles, F. F., Saraiva, A. A. F., Staniczek, A. H., and Rodrigues, T. (2021a). An overview of the Hexagenitidae (Ephemeroptera) from the Crato Formation (Aptian, Lower Cretaceous) of Brazil, with the description of a new species. *Historical Biol.* 34, 875–884. doi: 10.1080/08912963.2021.1952196

Storari, A. P., Osés, G. L., Almeida-Lima, D. S. D., Rizzutto, M. A., Bantim, R. A. M., Lima, F. J., et al. (2024). Exceptionally well-preserved orthopteran proventriculi from the Cretaceous Crato Formation of Brazil. *J. South Am. Earth Sci.* 133, 104737. doi: 10.1016/j.jsames.2023.104737

Storari, A. P., Rodrigues, T., Bantim, R. A. M., Lima, F. J., and Saraiva, A. A. F. (2021b). Mass mortality events of autochthonous faunas in a Lower Cretaceous Gondwanan Lagerstätte. *Sci. Rep.* 11, 6976. doi: 10.1038/s41598-021-85953-5

Storari, A. P., Rodrigues, T., Saraiva, A. A. F., and Salles, F. F. (2020). Unmasking a Gap: A New Oligoneuriid Fossil (Ephemeroptera: Insecta) from the Crato Formation (Upper Aptian), Araripe Basin, NE Brazil, with Comments on Colocrus McCafferty. *PLOS ONE* 15 (10), e0240365. doi: 10.1371/journal.pone.0240365

Tałanda, M. (2018). An exceptionally preserved Jurassic skink suggests lizard diversification preceded fragmentation of Pangaea. *Palaeontology* 61, 659–677. doi: 10.1111/pala.12358

Tischlinger, H. (2001). Bemerkungen zur Insekten-Taphonomie der Solnhofener Plattenkalke. *Archaeopteryx* 19, 29–44.

Tischlinger, H., and Unwin, D. (2004). UV-Untersuchungen des Berliner Exemplars von *Archaeopteryx lithographica* H.v.Meyer 1861 und der isolierten *Archaeopteryx*-Feder. *Archaeopteryx* 22, 17–50.

Varejão, F. G., Warren, L. V., Simões, M. G., Buatois, L. A., Angano, G. M., and Bahniuk- Rumbelsperger, A. N. (2021). Mixed siliciclastic–carbonate sedimentation in an evolving epicontinental sea: Aptian record of marginal marine settings in the interior basins of north-eastern Brazil. *Sedimentology* 68, 2125–2164. doi: 10.1111/sed.12846

Varejão, F. G., Warren, L. V., Simões, M. G., Fürsich, F. T., Matos, S. A., and Assine, M. L. (2019). Exceptional preservation of soft tissues by microbial entombment: Insights into the taphonomy of the Crato Konservat-Lagerstätte. *Palaios* 34, 331–348. doi: 10.2110/palo.2019.041

Viana, M. S., and Neumann, V. H. L. (2002). "Membro Crato da Formação Santana, Chapada do Araripe, CE - Riquíssimo registro de fauna e flora do Cretáceo," in *Sítios Geológicos e Paleontológicos do Brasil*. Eds. C. Schobbenhaus, D. A. Campos, E. T. Queiroz, M. Winge and M. L. C. Berbert-Born (DNPM/CPRM - Comissão Brasileira de Sítios Geológicos e Paleobiológicos, 113-120).

Viohl, G. (1990). "Taphonomy of fossil-lagerstätten. Solnhofen lithographic limestones," in *Palaeobiology. A synthesis*. Eds. D. E. G. Briggs and P. R. Crowther (Blackwell, Oxford), 285–289.

Viohl, G. (1994). Fish taphonomy of the Solnhofen Plattenkalk. An approach to the reconstruction of paleoenvironment. *Géo. Mém. Spéc.* 16, 81–90. doi: 10.1016/S0016-6995(94)80023-5

Viohl, G. (2015). "Die Plattenkalk-Typen der süadlichen Frankenalb," in *Solnhofen. Ein Fenster in die Jurazeit*. Eds. G. Arratia, H. P. Schultze, H. Tischlinger and G. Viohl (Verlag Dr. Friedrich Pfeil, Munich), 72–77.

Wang, B., Zhang, H. C., Wappler, T., and Rust, J. (2010). Palaeontinidae (Insecta: Hemiptera: Cicadomorpha) from the Upper Jurassic Solnhofen Limestone of Germany and their phylogenetic significance. *Geological Magazine* 147, 570–580. doi: 10.1017/s0016756809990896

Wang, B., Zhao, F., Zhang, H., Fang, Y., and Zheng, D. (2012). Widespread pyritization of insects in the Early Cretaceous Jehol biota. *Palaios* 27, 707–711. doi: 10.2110/palo.2012.p12-029r

Wappler, T., and Ben-Dov, Y. (2008). Preservation of armoured scale insects on angiosperm leaves from the eocene of Germany. *Acta Palaeontologica Polonica* 53, 627–634. doi: 10.4202/app.2008.0407

Warren, L. V., Varejão, F. G., Quaglio., F., Simões., M. G., Fürsich, F. T., Poiré, D. G., et al. (2016). Stromatolites from the Aptian Crato Formation, a hypersaline lake system in the Araripe Basin, northeastern Brazil. *Facies* 63 (3). doi: 10.1007/s10347-016-0484-6

Wilby, P. R., and Briggs, D. E. G. (1997). Taxonomic trends in the resolution of detail preserved in fossil phosphatized soft-tissues. *Geobios* 20, 493e502. doi: 10.1016/S0016-6995(97)80056-3